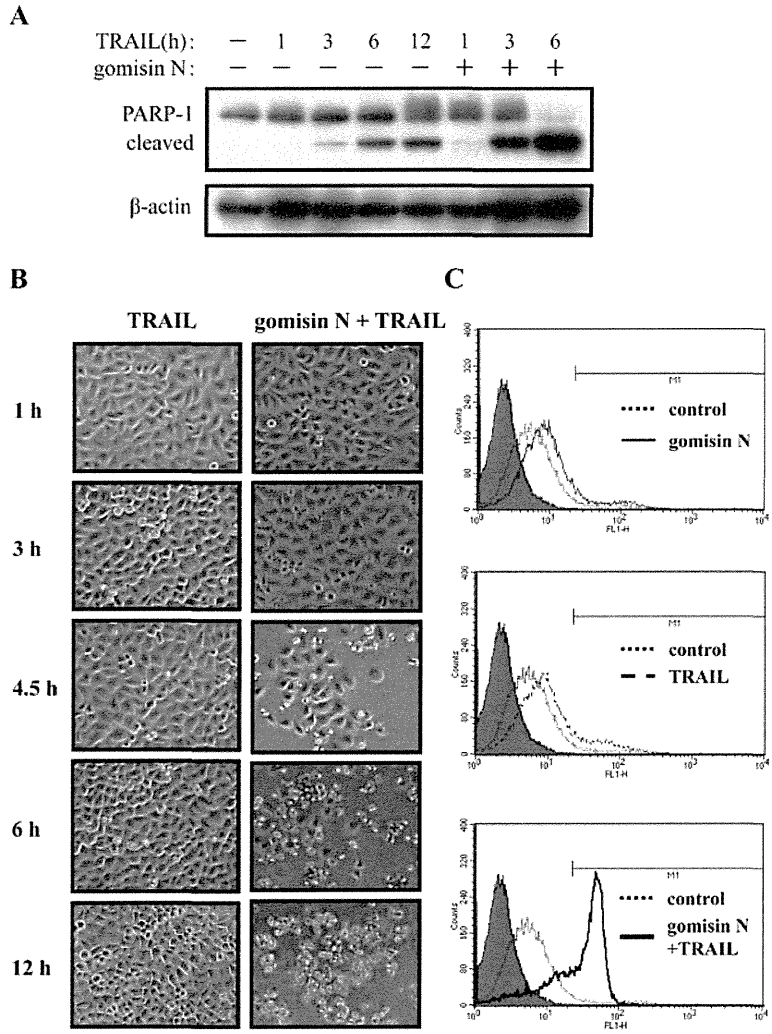

Figure 2. Pretreatment with gomisin N promotes TRAIL-mediated apoptosis. (A) Hela cells were pretreated with 100 μM gomisin N for 30 min and then treated with TRAIL (100 ng/ml) for the indicated hours. Cell lysates were collected and subjected to Western blot analysis to detect the cleavage of PARP-1. (B) Gomisin N morphologically enhanced the cell death induced by TRAIL in HeLa cells. Left, cells treated with TRAIL for the indicated hours; right, cells pretreated with gomisin N for 30 min, followed by TRAIL for the indicated hours. Representative images of cells were photographed using a normal light microscope. Magnification, x100. (C) Cells were treated with gomisin N for 30 min, followed by TRAIL for 6 h. Cells were stained with Annexin V-FITC and analyzed by FACS.

were treated with TRAIL (100 ng/ml) for 2.5 h. The cells were stained with 5 μM CMH_2DCFDA for 30 min at 37˚C and harvested, and fluorescence intensity was analyzed using the FACSCalibur System (BD Biosciences).

Statistical analysis. All values are presented as the mean ± SD and were analyzed by one-way analysis of variance (ANOVA) followed by the Tukey-Kramer test. $P<0.05$ was accepted as significant.

Results

Gomisin N augments TRAIL-induced apoptosis in HeLa cells. Gomisins have been shown to induce apoptosis in cancer cells. We first confirmed the effects of gomisins A and N on TRAIL-induced apoptosis in HeLa cells. Gomisin A alone did not cause evident degradation of PARP-1, an important marker of apoptosis, and gomisin N and TRAIL alone induced cleavage of PARP-1 weakly, however, gomisin N, but not gomisin A, significantly enhanced TRAIL-induced cleavage of caspase-3 and PARP-1 (Fig. 1A). As shown in Fig. 1B, although gomisin N showed slight inhibition at a concentration of 100 μM, gomisin N enhanced TRAIL-induced cell death in a concentration-dependent manner. When treated with TRAIL alone at 100 ng/ml, cleavage of PARP-1 was detected in a time-dependent manner, and pretreatment with gomisin N accelerated TRAIL-induced cleavage of PARP-1 (Fig. 2A). Morphological changes were also observed after treatment with gomisin N and TRAIL together (Fig. 2B). The flow cytogram of Annexin V analysis is shown in Fig. 2C. For the control group, the percentage of apoptotic cells was 4.4%. After treatment with TRAIL or gomisin N alone, the percentage of Annexin V-positive cells was 14.7 or 10.1%, respectively, however, after co-treatment with gomisin N and TRAIL, the percentage of apoptotic cells markedly increased to 66.1%. These results indicated that gomisin N enhanced TRAIL-induced apoptosis.

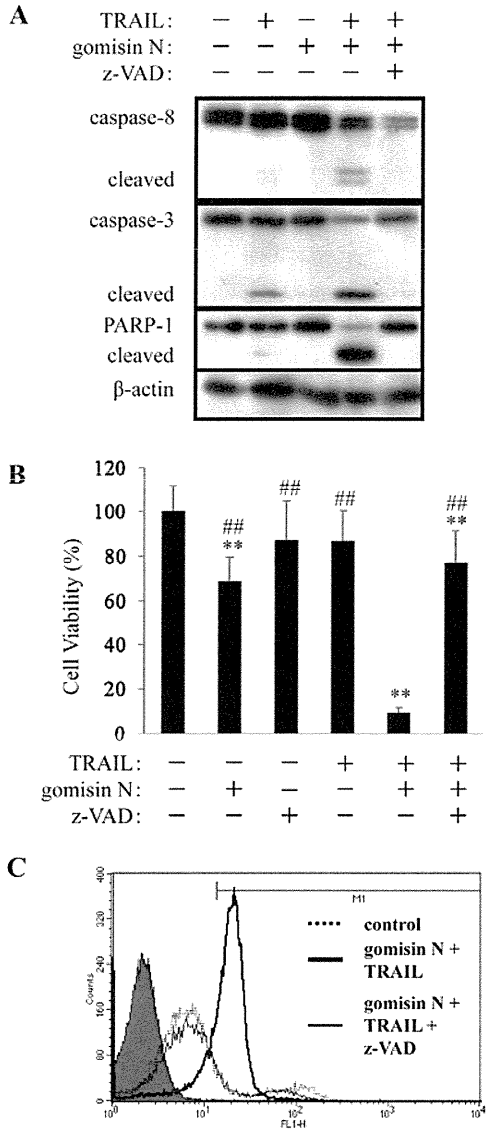

Figure 3. Combined treatment with gomisin N and TRAIL induces typical caspase-dependent apoptosis. (A) HeLa cells were pretreated with 10 μM z-VAD-FMK (z-VAD) for 30 min, followed by combined treatment with gomisin N (100 μM) for 30 min and then TRAIL (100 ng/ml) for another 3 h. Cells were collected to detect the cleavage of caspase-3, caspase-8 and PARP-1 by Western blot analysis. (B) HeLa cells were pretreated with z-VAD-FMK and gomisin N in a similar way and then treated with TRAIL for another 24 h. Cell viability was determined by WST-1 assay. Data are presented as the mean ± SD of six independent experiments; **P<0.01 vs. control group; $^{\#\#}$P<0.01 vs. combined treatment group with gomisin N and TRAIL. (C) HeLa cells were pretreated with z-VAD-FMK and gomisin N in a similar way and then treated with TRAIL for another 3 h. Cells were stained with Annexin V-FITC and analyzed by FACS.

TRAIL-induced apoptosis is promoted by gomisin N through the caspase cascade. Previous reports indicate that TRAIL-induced apoptosis is mainly executed through the extrinsic apoptosis pathway, involving caspase-8 and caspase-3 (20). We first examined the effect of gomisin N on TRAIL-induced activation of the caspase cascade. Fig. 3A shows that gomisin N alone had no effect on the degradation of caspase-8, caspase-3 and PARP-1, however, pretreatment with gomisin N significantly enhanced TRAIL-induced cleavage of caspase-8, caspase-3 and PARP-1. Moreover, pretreatment with z-VAD-FMK, a pan-caspase inhibitor, completely inhibited cleavage of caspase-8, caspase-3 and PARP-1 (Fig. 3A). In addition, WST-1 and Annexin V analyses showed that z-VAD-FMK also inhibited apoptosis induced by the combined treatment with gomisin N and TRAIL (Fig. 3B and C). These results suggested that gomisin N was able to promote TRAIL-induced apoptosis through the caspase cascade involving caspase-8 and caspase-3.

Gomisin N enhances TRAIL-induced apoptosis via up-regulation of DR4 and DR5. It is well documented that decreased expression of TRAIL receptors DR4 and DR5 or increased expression of the decoy receptors DcR1 and DcR2 are responsible for TRAIL resistance in several cancer cell lines (13,20-22). To explore the underlying mechanism by which gomisin N enhanced TRAIL-induced apoptosis, we first detected the mRNA levels of DR4 and DR5 in HeLa cells treated with gomisin N. As shown in Fig. 4A, gomisin N significantly up-regulated the expression of DR4 and DR5 mRNA, and the combination of gomisin N and TRAIL accelerated the expression of DR4 and DR5. Furthermore, although TRAIL did not up-regulate mRNA levels of DR4 and DR5, gomisin N up-regulated DR4 and DR5 expression in a time-dependent manner until 6 h (Fig. 4B). Next to confirm the roles of DR4 and DR5 in TRAIL-induced apoptosis, TRAIL receptors were neutralized by anti-DR4 and DR5 blocking antibodies. As shown in Fig. 4C, WST-1 analysis demonstrated that DR4 blocking antibody was not able to inhibit TRAIL-induced cell death, however, after the neutralization of DR5, the percentage of cell viability increased to 23%. Moreover, after neutralizing both DR4 and DR5, the percentage increased to 37%. Western blot analysis showed that DR4 and DR5 blocking antibodies could inhibit the degradation of caspase-8, caspase-3 and PARP-1 similarly (Fig. 4D). These results suggested that gomisin N up-regulated DR4 and DR5 expression at the transcriptional level, and not only up-regulation of DR5 but also that of DR4 might be one of the mechanisms in the sensitization of TRAIL-induced apoptosis by gomisin N.

Gomisin N up-regulates DR4 and DR5 expression by increasing ROS. It has been reported that several natural products have ROS-generating activity and ROS are related to the up-regulation of TRAIL receptors (23-25). Here, we measured intracellular ROS levels treated with gomisin N. As shown in Fig. 5A, after treatment with TRAIL alone, the intracellular ROS level was almost the same as that of control cells without stimulation; however, after treatment with gomisin N, the ROS level increased significantly and co-treatment with gomisin N and TRAIL accelerated ROS production. Moreover, pretreatment with N-acetyl cysteine (NAC), an antioxidant, markedly reduced ROS production (Fig. 5B) and also significantly inhibited up-regulation of DR4 and DR5 induced by gomisin N (Fig. 5C). These findings indicated that up-regulation of DR4 and DR5 induced by gomisin N was dependent on ROS generation.

Gomisin N does not markedly affect the mRNA expression of TRAIL decoy receptors, and protein expression of the intrinsic apoptosis pathway. To investigate whether TRAIL decoy receptors were relevant to the sensitization of TRAIL-induced

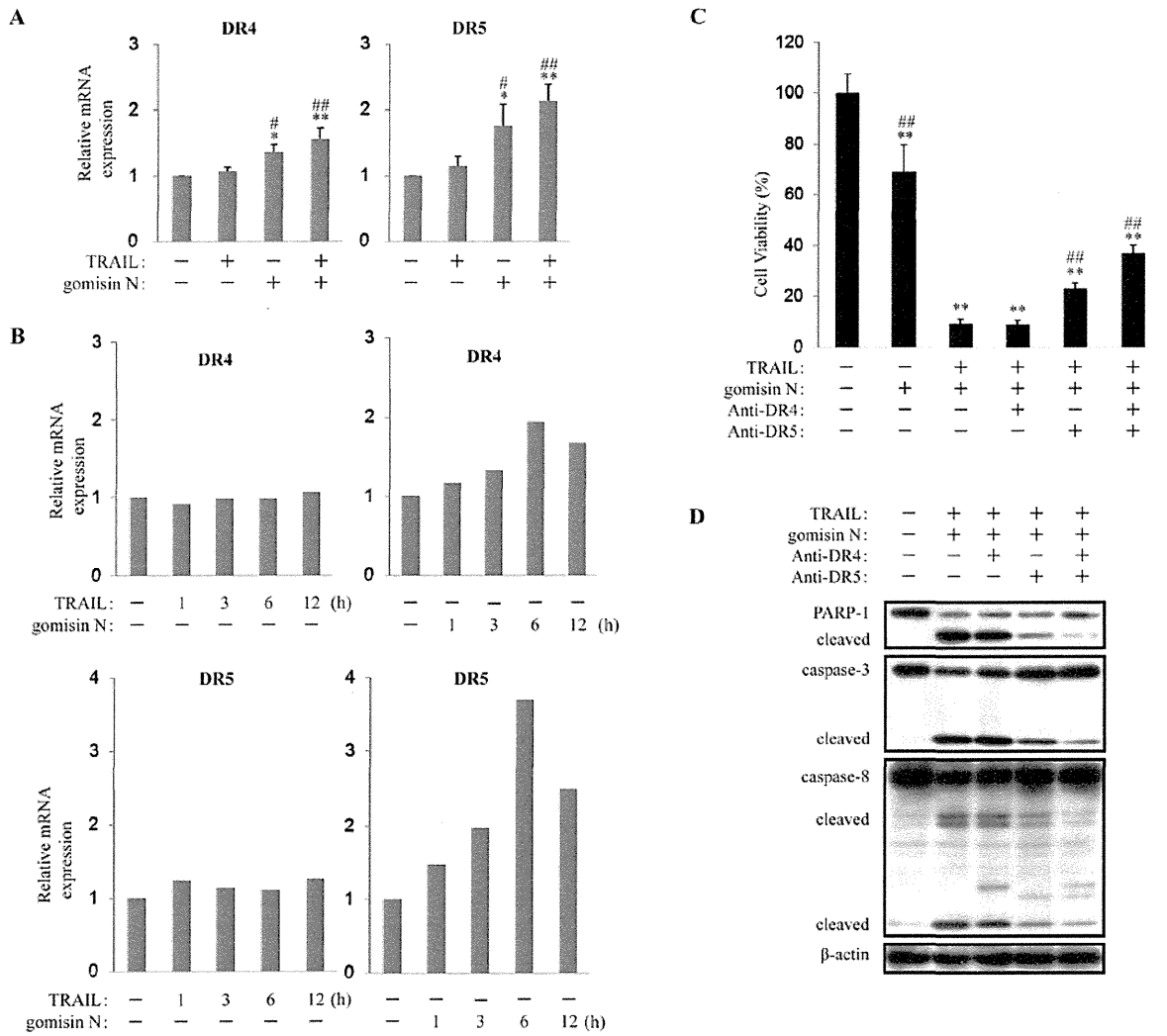

Figure 4. Gomisin N up-regulates mRNA expression of DR4 and DR5. (A) HeLa cells were pretreated with gomisin N (100 μM) for 30 min, followed by TRAIL (100 ng/ml) for 3 h. The mRNA levels of DR4 and DR5 were measured by real-time RT-PCR. Data are presented as the mean ± SD of three independent experiments; *P<0.05, **P<0.01 vs. control group, $^{\#}$P<0.05, $^{\#\#}$P<0.01 vs. treatment group with TRAIL. (B) HeLa cells were treated with TRAIL for the indicated hours (left). HeLa cells were pretreated with gomisin N for 30 min, followed by TRAIL for the indicated hours (right). The mRNA levels of DR4 and DR5 were measured by real-time RT-PCR. (C) HeLa cells were pretreated with DR4 and/or DR5 blocking antibodies (10 μg/ml) for 30 min, followed by combined treatment with gomisin N for 30 min and then TRAIL for another 24 h. Cell viability was determined by WST-1 assay. Data are presented as the mean ± SD of six independent experiments; **P<0.01 vs. control group; $^{\#\#}$P<0.01 vs. combined treatment group with gomisin N and TRAIL. (D) HeLa cells were pretreated with DR4 and/or DR5 blocking antibodies and gomisin N in a similar way and then treated with TRAIL for another 3 h. Cells were collected for detecting the cleavage of caspase-3, caspase-8 and PARP-1 by Western blotting.

apoptosis by gomisin N, we examined mRNA expression of DcR1 and DcR2. As shown in Fig. 6A, gomisin N did not change the expression of DcR1 and DcR2. We also examined the protein levels of the intrinsic apoptosis pathway. Bcl-2, Bcl-xL, XIAP, cytochrome c and caspase-9 were not significantly changed by gomisin N treatment in HeLa cells (Fig. 6B). These findings suggested that gomisin N did not affect the mRNA expression of TRAIL decoy receptors and the intrinsic apoptosis pathway.

Discussion

The effectiveness of chemotherapeutic drugs in cancer treatment has been limited by systemic toxicity and drug resistance. The distinct ability of triggering apoptosis in many types of human cancer cells while sparing normal cells makes TRAIL an attractive agent for cancer therapy, however, resistance to TRAIL-mediated apoptosis in cancer cells is a limitation in its clinical application as a cancer therapeutic agent. Thus, researchers are currently seeking TRAIL sensitizers to overcome resistance to TRAIL in cancer cells (18). A number of chemical compounds, including some natural products, have been identified as effective sensitizing agents to TRAIL-induced apoptosis (23,26-36). Gomisin N, a dibenzocyclooctadiene lignan isolated from the fruit of *S. chinensis*, has been reported as an anticancer drug candidate. Recent study demonstrated that gomisin N inhibited proliferation and induced apoptosis in human hepatic carcinomas (10). We have shown that gomisin N could sensitize TNF-α-induced apoptosis in HeLa cells (11), and the findings from this study provided substantial evidence that gomisin N was also capable of sensitizing TRAIL-induced apoptosis in HeLa cells. Thus,

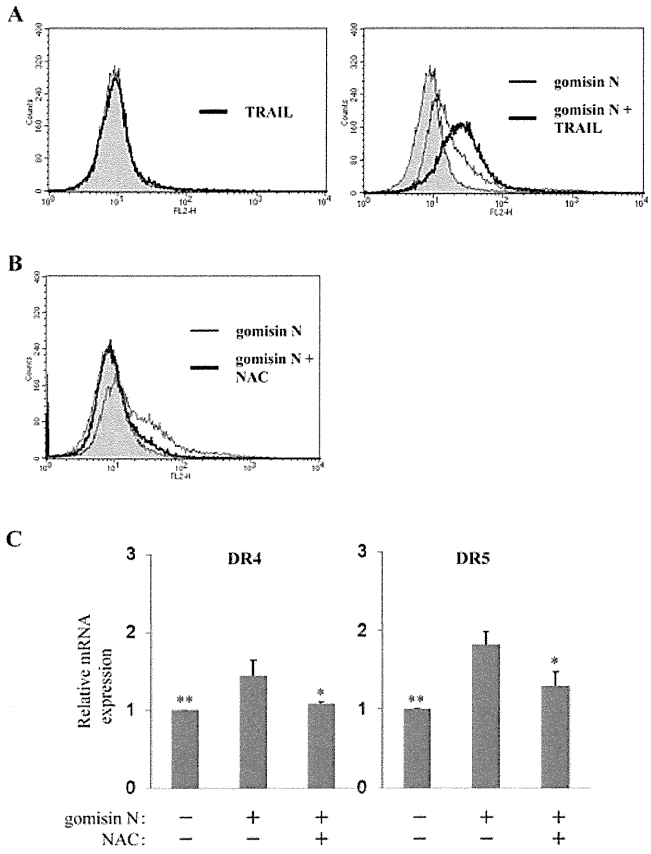

Figure 5. Gomisin N induces generation of ROS and up-regulation of DR4 and DR5 is dependent on ROS generation. (A) HeLa cells were pretreated with gomisin N (100 μM) for 30 min, followed by treatment with TRAIL (100 ng/ml) for 2.5 h. Cells were stained with 5 μM CMH_2DCFDA for 30 min and analyzed by FACS. (B) HeLa cells were pretreated with 5 mM NAC for 30 min, followed by treatment with gomisin N for 3 h. Cells were stained with 5 μM CMH_2DCFDA for 30 min and analyzed by FACS. (C) HeLa cells were treated with NAC (5 mM) followed by treatment with gomisin N for 3.5 h. The mRNA levels of DR4 and DR5 were measured by real-time RT-PCR. Data are presented as the mean ± SD of three independent experiments; $^{*}P<0.05$, $^{**}P<0.01$ vs. treatment group with gomisin N.

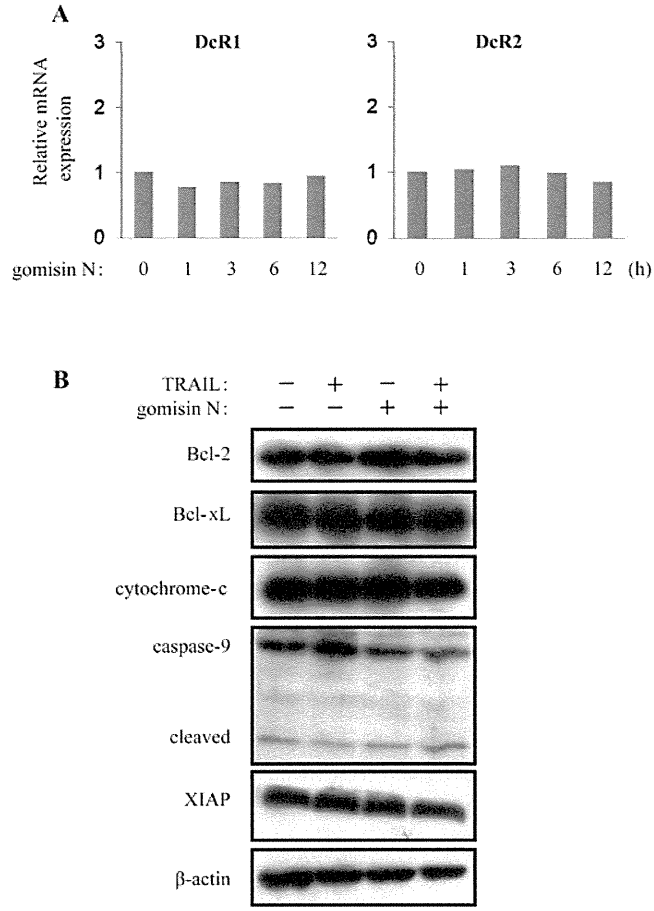

Figure 6. Effect of gomisin N on TRAIL decoy receptors and various apoptosis regulatory proteins. (A) HeLa cells were treated with gomisin N (100 μM) for the indicated hours. The mRNA levels of DcR1 and DcR2 were measured by real-time RT-PCR. (B) HeLa cells were pretreated with gomisin N for 30 min, followed by treatment with TRAIL (100 ng/ml) for 3 h. Cell lysates were collected and subjected to Western blot analysis to detect apoptosis regulatory proteins.

this study presents a novel anticancer effect of gomisin N and enhances the possibility of TRAIL in clinical application.

In the present study, to explore TRAIL sensitivity in human cervical cancer cells, HeLa cells were treated with 100 ng/ml TRAIL for 24 h. As shown in Fig. 1B, the viability of HeLa cells treated with TRAIL alone was 81%, but when treated with gomisin N (100 μM) and TRAIL, the percentage of viability decreased significantly to 7%. Analyses of apoptotic cells by Annexin V-FITC are shown in Fig. 2C. It was revealed that cells induced to undergo apoptosis by TRAIL alone were only 14.7%, but after treatment with gomisin N and TRAIL, the percentage of apoptotic cells increased to 66.1%. These results suggested that HeLa cells were resistant to TRAIL-induced apoptosis and gomisin N could promote TRAIL-induced apoptosis. To clarify the signaling pathway of apoptosis induced by TRAIL, we characterized the caspase-dependent pathway. The activation of caspase-8, caspase-3 and PARP-1 confirmed that the cell death induced by gomisin N and TRAIL was caspase-dependent apoptosis. As shown in Fig. 3, the pan-caspase inhibitor (z-VAD-FMK) was able to prevent PARP-1 cleavage and apoptosis induced by combined treatment with gomisin N and TRAIL, therefore, it was clarified that the apoptosis induced by gomisin N and TRAIL was caspase-dependent. Gomisin A enhanced the cleavage of PARP-1 induced by TRAIL slightly, but did not augment the cleavage of caspase-3 induced by TRAIL (Fig. 1A), therefore it was necessary to investigate the molecular mechanisms of gomisin A in enhancing the cleavage of PARP-1.

The expression level of death receptors (DR4 or DR5) plays a key role in determining the cell fate in response to TRAIL (20-22). There are numerous reports that the up-regulation of DR4 or DR5 could sensitize TRAIL-resistant cells to TRAIL-induced cell death (37,38). In this study, we showed for the first time that gomisin N increased DR4 and DR5 expression in HeLa cells (Fig. 4A and B). When we neutralized only DR4 by using a blocking antibody, the percentage of cell viability was not recovered, as compared with that of the combination of gomisin N and TRAIL. However, pretreatment with both DR4 and DR5 blocking antibodies inhibited the cell death induced by gomisin N and TRAIL more strongly than that of only DR5 (Fig. 4C), so we believed that both DR4 and DR5 up-regulated by gomisin N played key roles in sensitizing HeLa cells to TRAIL-induced apoptosis.

ROS generation has been proposed to be involved in the up-regulation of TRAIL receptors (23-25). The present study revealed that the mechanism by which gomisin N induced up-regulation of DR4 and DR5 was through the production of ROS. The antioxidant (NAC) could abolish the up-regulation of TRAIL receptors by gomisin N (Fig. 5C), therefore ROS production led to the up-regulation of DR4 and DR5, caspase cascade and eventually enhanced cell death.

In summary, we showed that gomisin N overcame TRAIL resistance through ROS-mediated up-regulation of DR4 and DR5 expression. Gomisin N might be useful to increase TRAIL efficacy in the treatment of malignant tumors.

Acknowledgements

This study was supported in part by Grants-in-Aid for Challenging Exploratory Research (No. 09002374) and Scientific Research (C) (No. 23590071) from the Ministry of Education, Culture, Sports, Science and Technology (MEXT), Japan and a grant from the First Bank of Toyama Foundation.

References

1. Sterbova H, Sevcikova P, Kvasnickova L, Glatz Z and Slanina J: Determination of lignans in *Schisandra chinensis* using micellar electrokinetic capillary chromatography. Electrophoresis 23: 253-258, 2002.
2. He X, Lian L and Lin L: Analysis of lignan constituents from *Schisandra chinensis* by liquid chromatography-electrospray mass spectrometry. J Chromatogr A 757: 81-87, 1997.
3. Min HY, Park EJ, Hong JY, Kang YJ, Kim SJ, Chung HJ, Woo ER, Hung TM, Youn UJ, Kim YS, Kang SS, Bae K and Lee SK: Antiproliferative effects of dibenzocyclooctadiene lignans isolated from *Schisandra chinensis* in human cancer cells. Bioorg Med Chem Lett 18: 523-526, 2008.
4. Choi MS, Kwon KJ, Jeon SJ, Go HS, Kim KC, Ryu JR, Lee JM, Han SH, Cheong JH, Ryu JH, Shin KH and Ko CY: *Schizandra chinensis* alkaloids inhibit lipopolysaccharide-induced inflammatory responses in BV2 microglial cells. J Biomol Tech 17: 47-56, 2009.
5. Oh SY, Kim YH, Bae DS, Um BH, Pan CH, Kim CY, Lee HJ and Lee JK: Anti-inflammatory effects of gomisin N, gomisin J, and schisandrin C isolated from the fruit of *Schisandra chinensis*. Biosci Biotechnol Biochem 74: 285-291, 2010.
6. Marek J and Slanina J: Gomisin N. Acta Cryst 54: 1548-1550, 1998.
7. Opletal L, Sovova H and Bartlova M: Dibenzo[a,c]cyclooctadiene lignans of the genus *Schisandra*: importance, isolation and determination. J Chromatogr B Analyt Technol Biomed Life Sci 812: 357-371, 2004.
8. Choi YW, Takamatsu S, Khan SI, Srinivas PV, Ferreira D, Zhao J and Khan IA: Schisandrene, a dibenzocyclooctadiene lignan from *Schisandra chinensis*: structure-antioxidant activity relationships of dibenzocyclooctadiene lignans. J Nat Prod 69: 356-359, 2006.
9. Kim SH, Kim YS, Kang SS, Bae K, Hung TM and Lee SM: Anti-apoptotic and hepatoprotective effects of gomisin A on fulminant hepatic failure induced by D-galactosamine and lipopolysaccharide in mice. J Pharmacol Sci 106: 225-233, 2008.
10. Yim SY, Lee YJ, Lee YK, Jung SE, Kim JH, Kim HJ, Son BG, Park YH, Lee YG, Choi YW and Hwang DY: Gomisin N isolated from *Schisandra chinensis* significantly induces antiproliferative and pro-apoptotic effects in hepatic carcinoma. Mol Med Rep 2: 725-732, 2009.
11. Waiwut P, Shin MS, Inujima A, Zhou Y, Koizumi K, Saiki I and Sakurai H: Gomisin N enhances TNF-α-induced apoptosis via inhibition of the NF-κB and EGFR survival pathways. Mol Cell Biochem 350: 169-175, 2011.
12. Mahmood Z and Shukla Y: Death receptors: targets for cancer therapy. Exp Cell Res 316: 887-899, 2010.
13. Wu GS: TRAIL as a target in anti-cancer therapy. Cancer Lett 285: 1-5, 2009.
14. Ashkenazi A, Pai RC, Fong S, Leung S, Lawrence DA, Marsters SA, Blackie C, Chang L, McMurtrey AE, Hebert A, DeForge L, Koumenis IL, Lewis D, Harris L, Bussiere J, Koeppen H, Shahrokh Z and Schwall RH: Safety and antitumor activity of recombinant soluble Apo2 ligand. J Clin Invest 104: 155-162, 1999.
15. Shankar S and Srivastava RK: Enhancement of therapeutic potential of TRAIL by cancer chemotherapy and irradiation: mechanisms and clinical implications. Drug Resist Updat 7: 139-156, 2004.
16. Sheridan JP, Marsters SA, Pitti RM, Gurney A, Skubatch M, Baldwin D, Ramakrishnan L, Gray CL, Baker K, Wood WI, Goddard AD, Godowski P and Ashkenazi A: Control of TRAIL-induced apoptosis by a family of signaling and decoy receptors. Science 277: 818-821, 1997.
17. MacFarlane M: TRAIL-induced signalling and apoptosis. Toxicol Lett 139: 89-97, 2003.
18. Zhang L and Fang B: Mechanisms of resistance to TRAIL-induced apoptosis in cancer. Cancer Gene Ther 12: 228-237, 2005.
19. Fandy TE and Srivastava RK: Trichostatin A sensitizes TRAIL-resistant myeloma cells by downregulation of the antiapoptotic Bcl-2 proteins. Cancer Chemother Pharmacol 58: 471-477, 2006.
20. LeBlanc HN and Ashkenazi A: Apo2L/TRAIL and its death and decoy receptors. Cell Death Differ 10: 66-75, 2003.
21. Wang S and El-Deiry WS: TRAIL and apoptosis induction by TNF-family death receptors. Oncogene 22: 8628-8633, 2003.
22. Takeda K, Stagg J, Yagita H, Okumura K and Smyth MJ: Targeting death-inducing receptors in cancer therapy. Oncogene 26: 3745-3757, 2007.
23. Zhou J, Lu GD, Ong CS, Ong CN and Shen HM: Andrographolide sensitizes cancer cells to TRAIL-induced apoptosis via p53-mediated death receptor 4 up-regulation. Mol Cancer Ther 7: 2170-2180, 2008.
24. Taniguchi H, Yoshida T, Horinaka M, Yasuda T, Goda AE, Konishi M, Wakada M, Kataoka K, Yoshikawa T and Sakai T: Baicalein overcomes tumor necrosis factor-related apoptosis-inducing ligand resistance via two different cell-specific pathways in cancer cells but not in normal cells. Cancer Res 68: 8918-8927, 2008.
25. Prasad S, Ravindran J, Sung B, Pandey MK and Aggarwal BB: Garcinol potentiates TRAIL-induced apoptosis through modulation of death receptors and antiapoptotic proteins. Mol Cancer Ther 9: 856-868, 2010.
26. Li X, Wang JN, Huang JM, Xiong XK, Chen MF, Ong CN, Shen HM and Yang XF: Chrysin promotes tumor necrosis factor (TNF)-related apoptosis-inducing ligand (TRAIL) induced apoptosis in human cancer cell lines. Toxicol In Vitro 25: 630-635, 2011.
27. Lee DH, Rhee JG and Lee YJ: Reactive oxygen species up-regulate p53 and Puma; a possible mechanism for apoptosis during combined treatment with TRAIL and wogonin. Br J Pharmacol 157: 1189-1202, 2009.
28. Ishiguro K, Ando T, Maeda O, Ohmiya N, Niwa Y, Kadomatsu K and Goto H: Ginger ingredients reduce viability of gastric cancer cells via distinct mechanisms. Biochem Biophys Res Commun 362: 218-223, 2007.
29. Frese S, Pirnia F, Miescher D, Krajewski S, Borner MM, Reed JC and Schmid RA: PG490-mediated sensitization of lung cancer cells to Apo2L/TRAIL-induced apoptosis requires activation of ERK2. Oncogene 22: 5427-5435, 2003.
30. Lee KY, Park JS, Jee YK and Rosen GD: Triptolide sensitizes lung cancer cells to TNF-related apoptosis-inducing ligand (TRAIL)-induced apoptosis by inhibition of NF-kappaB activation. Exp Mol Med 34: 462-468, 2002.
31. Inoue S, MacFarlane M, Harper N, Wheat LM, Dyer MJ and Cohen GM: Histone deacetylase inhibitors potentiate TNF-related apoptosis-inducing ligand (TRAIL)-induced apoptosis in lymphoid malignancies. Cell Death Differ 11 (Suppl 2): S193-S206, 2004.
32. Palacios C, Yerbes R and Lopez-Rivas A: Flavopiridol induces cellular FLICE-inhibitory protein degradation by the proteasome and promotes TRAIL-induced early signaling and apoptosis in breast tumor cells. Cancer Res 66: 8858-8869, 2006.
33. Ganten TM, Koschny R, Haas TL, Sykora J, Li-Weber M, Herzer K and Walczak H: Proteasome inhibition sensitizes hepatocellular carcinoma cells, but not human hepatocytes, to TRAIL. Hepatology 42: 588-597, 2005.

34. Shi RX, Ong CN and Shen HM: Protein kinase C inhibition and x-linked inhibitor of apoptosis protein degradation contribute to the sensitization effect of luteolin on tumor necrosis factor-related apoptosis-inducing ligand-induced apoptosis in cancer cells. Cancer Res 65: 7815-7823, 2005.
35. Zhang S, Shen HM and Ong CN: Down-regulation of c-FLIP contributes to the sensitization effect of 3,3'-diindolylmethane on TRAIL-induced apoptosis in cancer cells. Mol Cancer Ther 4: 1972-1981, 2005.
36. Son YG, Kim EH, Kim JY, Kim SU, Kwon TK, Yoon AR, Yun CO and Choi KS: Silibinin sensitizes human glioma cells to TRAIL-mediated apoptosis via DR5 up-regulation and down-regulation of c-FLIP and survivin. Cancer Res 67: 8274-8284, 2007.
37. Galligan L, Longley DB, McEwan M, Wilson TR, McLaughlin K and Johnston PG: Chemotherapy and TRAIL-mediated colon cancer cell death: the roles of p53, TRAIL receptors, and c-FLIP. Mol Cancer Ther 4: 2026-2036, 2005.
38. Jin Z, McDonald ER III, Dicker DT and El-Deiry WS: Deficient tumor necrosis factor-related apoptosis-inducing ligand (TRAIL) death receptor transport to the cell surface in human colon cancer cells selected for resistance to TRAIL-induced apoptosis. J Biol Chem 279: 35829-35839, 2004.

Hindawi Publishing Corporation
Evidence-Based Complementary and Alternative Medicine
Volume 2011, Article ID 348686, 9 pages
doi:10.1155/2011/348686

Research Article

Effect of Hachimijiogan against Renal Dysfunction and Involvement of Hypoxia-Inducible Factor-1α in the Remnant Kidney Model

Hiroshi Oka,[1] Hirozo Goto,[1] Keiichi Koizumi,[2,3] Shin Nakamura,[4] Koichi Tsuneyama,[5] Yue Zhou,[2] Michiko Jo,[3] Takako Fujimoto,[6] Hiroaki Sakurai,[2] Naotoshi Shibahara,[3] Ikuo Saiki,[2] and Yutaka Shimada[1]

[1] *Department of Japanese Oriental Medicine, Graduate school of Medicine and Pharmaceutical Sciences, University of Toyama, 2630 Sugitani, Toyama 930-0194, Japan*
[2] *Division of Pathogenic Biochemistry, Institute of Natural Medicine, University of Toyama, 2630 Sugitani, Toyama 930-0194, Japan*
[3] *Department of Kampo Diagnostics, Institute of Natural Medicine, University of Toyama, 2630 Sugitani, Toyama 930-0194, Japan*
[4] *Biomedical Institute, NPO Primate Agora, Inuyama, Aichi 484-0002, Japan*
[5] *Department of Diagnostic Pathology, Graduate School of Medicine and Pharmaceutical Sciences, University of Toyama, 2630 Sugitani, Toyama 930-0194, Japan*
[6] *Faculty of Human Development, University of Toyama, 3190 Gofuku, Toyama 930-8555, Japan*

Correspondence should be addressed to Hirozo Goto, hiro510@med.u-toyama.ac.jp

Received 2 November 2010; Accepted 7 January 2011

Copyright © 2011 Hiroshi Oka et al. This is an open access article distributed under the Creative Commons Attribution License, which permits unrestricted use, distribution, and reproduction in any medium, provided the original work is properly cited.

In chronic renal failure, hypoxia of renal tissue is thought to be the common final pathway leading to end-stage renal failure. In this study the effects of hachimijiogan, a Kampo formula, were studied with respect to hypoxia-inducible factor (HIF). Using remnant kidney rats, we studied the effects of hachimijiogan on renal function in comparison with angiotensin II receptor blocker. The result showed that oral administration of hachimijiogan for seven days suppressed urinary protein excretion and urinary 8-OHdG, a marker of antioxidant activity, equally as well as oral administration of candesartan cilexetil. In contrast, the protein volume of HIF-1α in the renal cortex was not increased in the candesartan cilexetil group, but that in the hachimijiogan group was increased. In immunohistochemical studies as well, the expression of HIF-1α of the high-dose hachimijiogan group increased compared to that of the control group. Vascular endothelial growth factor and glucose transporter 1, target genes of HIF-1α, were also increased in the hachimijiogan group. These results suggest that hachimijiogan produces a protective effect by a mechanism different from that of candesartan cilexetil.

1. Introduction

In recent years, it has been clear that chronic kidney disease (CKD) is an important risk factor for cardiovascular diseases and mortality and has been the focus of considerable attention [1]. The number of dialysis patients caused by end-stage renal disease has been increasing worldwide, regardless of the advances in treatments, such as a protein- and sodium-restricted diet, medicines containing angiotensin II receptor blocker (ARB), and kidney transplants [2]. There are various causes for the early stage of CKD, but there is a common pathway in advanced CKD as represented by interstitial fibrosis, glomerular sclerosis, and nephron destruction [3]. The kidney is sensitive to oxygen supply and is prone to sustaining damage from hypoxia. In recent years, it has been reported that chronic hypoxia in the kidney is the final common pathway to end-stage renal failure [4, 5]. Thus, therapeutic approaches against hypoxic injury in CKD patients are considered important for preventing the worsening of CKD. As a biological defense mechanism against tissue hypoxia, hypoxia-inducible factor (HIF), a heterodimeric transcription factor, plays an essential role. Activation of HIF stimulates numerous downstream target genes and protects tissue from hypoxia [6]. This effect is suggested by reports, which showed that cobalt ameliorates renal injury of renal disease model rats [7], and vascular

endothelial growth factor (VEGF) enhances glomerular capillary repair and accelerates resolution of experimentally induced glomerulonephritis [8].

Hachimijiogan, which we used in this study, is a Kampo formula created more than 1800 years ago. It is composed of eight crude drugs: Cinnamomi Cortex, Aconiti Japonici Tuber, Rehmanniae Radix, Corni Fructus, Dioscoreae Rhizoma, Alismatis Rhizoma, Moutan Cortex, and Hoelen. It has been clinically used to treat many symptoms, such as lumbago, pollakisuria, cold hands and feet, nephritis, and so on [9]. In basic research, it has been reported that hachimijiogan inhibits the progression of renal dysfunction in diabetic nephropathy model rats and 5/6 nephrectomized model rats. As the mechanism of its action, reduction of uremic toxins associated with antioxidant activity and positive effects on organic change of the kidney have been reported [10, 11].

However, there are no studies reporting the effect of hachimijiogan on HIF. Therefore, we examined the effect of hachimijiogan in comparison to ARB, a mainstream drug for renal disorder, on renal dysfunction from the aspect of hypoxic injury using 5/6 nephrectomized rats, in which tissue hypoxia causes progression of renal failure [12, 13].

2. Materials and Methods

2.1. Materials. The bulk extract of hachimijiogan (batch number 2060007020), which is approved for medical use in Japan, was purchased from Tsumura Co. Ltd. (Tokyo, Japan). It consists of eight herbs: 6.0 g of Rehmanniae Radix (*Rehmannia glutinosa* Liboschitz var. *purpurea* Makino), 3.0 g of Corni Fructus (*Cornus officinalis* Siebold et Zuccarini), 3.0 g of Dioscoreae Rhizoma (*Dioscorea japonica* Thunberg), 3.0 g of Alismatis Rhizoma (*Alisma orientale* Juzepczuk), 3.0 g of Hoelen (*Poria cocos* Wolf), 3.0 g of Moutan Cortex (*Paeonia suffruticosa* Andrews), 2.5 g of Cinnamomi Cortex (*Cinnamomum cassia* Blume), 1.0 g of Aconiti Tuber (*Aconitum carmichaeli* Debeaux).

Candesartan cilexetil was obtained from Takeda Pharmaceutical Company Ltd. (Osaka, Japan).

2.2. Three-Dimensional HPLC Analysis of Hachimijiogan. For analysis of the components of hachimijiogan, aqueous extract (1 g) was extracted with 20 mL methanol under ultrasonication for 30 min. The solution was filtered through a membrane filter (0.45 μm) and then subjected to high-performance liquid chromatography (HPLC) analysis using a TSK-GEL ODS-80TS column (φ4.6 × 250 mm, Tosoh, Tokyo, Japan) with an LC 10AD pump and an SPD-M10A absorbance detector. The elution solvents were (A) 0.05 M AcOH-$AcONH_4$ and (B) CH_3CN, and the column was eluted with a linear gradient of, by volume, 90% A and 10% B changing over 60 min to 100% B. The flow rate was 1.0 mL/min, and the effluent from the column was monitored and processed into three-dimensional data by an SPD-M10A array detector. All assigned peaks were identified by comparing their UV spectral data with those of coinjected authentic samples using the Class LC-10 Version 1.62 software package (Shimadzu, Kyoto, Japan). The three-dimensional HPLC profile of hachimijiogan extract is shown in Figure 1. The major components of hachimijiogan were morroniside, loganin, paeoniflorin, penta-O-galloyl glucose, benzoylmesaconine, benzoylpaeoniflorin, 16-ketoalisol A, paeonol, cinnamic acid, and cinnamaldehyde.

2.3. Animals and Treatments of Animals. All experimental procedures were performed in accordance with the standards established by the "Guide for the Care and Use of Laboratory Animals at the University of Toyama". Fifty 6-week-old male Sprague-Dawley rats were purchased from Japan SLC Inc. (Hamamatsu, Japan) and kept in an automatically controlled room (temperature about 23°C and humidity about 60%) with a conventional dark/light cycle. The animals were kept in metabolic cages, and 24-hour urine samples were collected. Blood pressure was determined by tail cuff system (MK2000, Muromachi Kikai Co., Ltd., Tokyo, Japan) in a conscious state. At 7 weeks old, 40 rats underwent 5/6 nephrectomy under anesthesia with sodium pentobarbital (50 mg/kg body weight, i.p.) by ablation of approximately 2/3 of the left kidney, and then removal of the right kidney by ligation of renal artery, vein, and ureter 1 week later. After recovery from the operation (after 1 week), the 5/6 nephrectomized (5/6Nx) rats were randomly divided into four groups (control and three treatment groups, n = 10/group). One more group of rats had undergone a sham operation (n = 10). During the experimental period, all groups were fed a standard chow. The sham and control groups were fed water, and the other three surgical groups were fed a solution of hachimijiogan extract orally at a dose of 220 mg/kg body weight/day (low-dose hachimijiogan), 660 mg/kg body weight/day (high-dose hachimijiogan), or a solution of candesartan cilexetil orally at a dose of 3 mg/kg body weight/day, respectively, by gastric gavage. These doses of hachimijiogan for rats were approximately 3 times and 10 times the human dose of hachimijiogan. After 7 days of treatment, the rats were sacrificed, and blood samples were obtained. The kidneys were removed from each rat, frozen quickly, and kept at −80°C until analysis.

2.4. Analysis of Serum and Urine Samples. Serum levels of Albumin were determined by SRL, Inc. (Tokyo, Japan). Serum levels of urea nitrogen (BUN) and creatinine (s-Cre) were determined using commercial kits (BUN Kainos and CRE-EN Kainos purchased from Kainos Laboratories, Inc., Tokyo, Japan). Urinary protein (u-Pro) excretion levels were determined using commercial reagents (Micro TP-test, Wako Pure Chemical, Osaka, Japan). Creatinine clearance (Ccr) was calculated on the basis of urinary creatinine, serum creatinine, urine volume, and body weight using the following equation: Ccr (mL/(kg body weight)/min) = {urinary Cre (mg/dL) × urine volume (mL)/serum Cre/(mg/dL)} × {1,000/body weight (g)} × {1/1,440 (min)}. 8-Hydroxy-deoxyguanosine (8-OHdG) content in 24-hour urine samples was measured by ELISA kit (8-OHdG Check, JaICA, Nikken SEIL Co., Shizuoka, Japan).

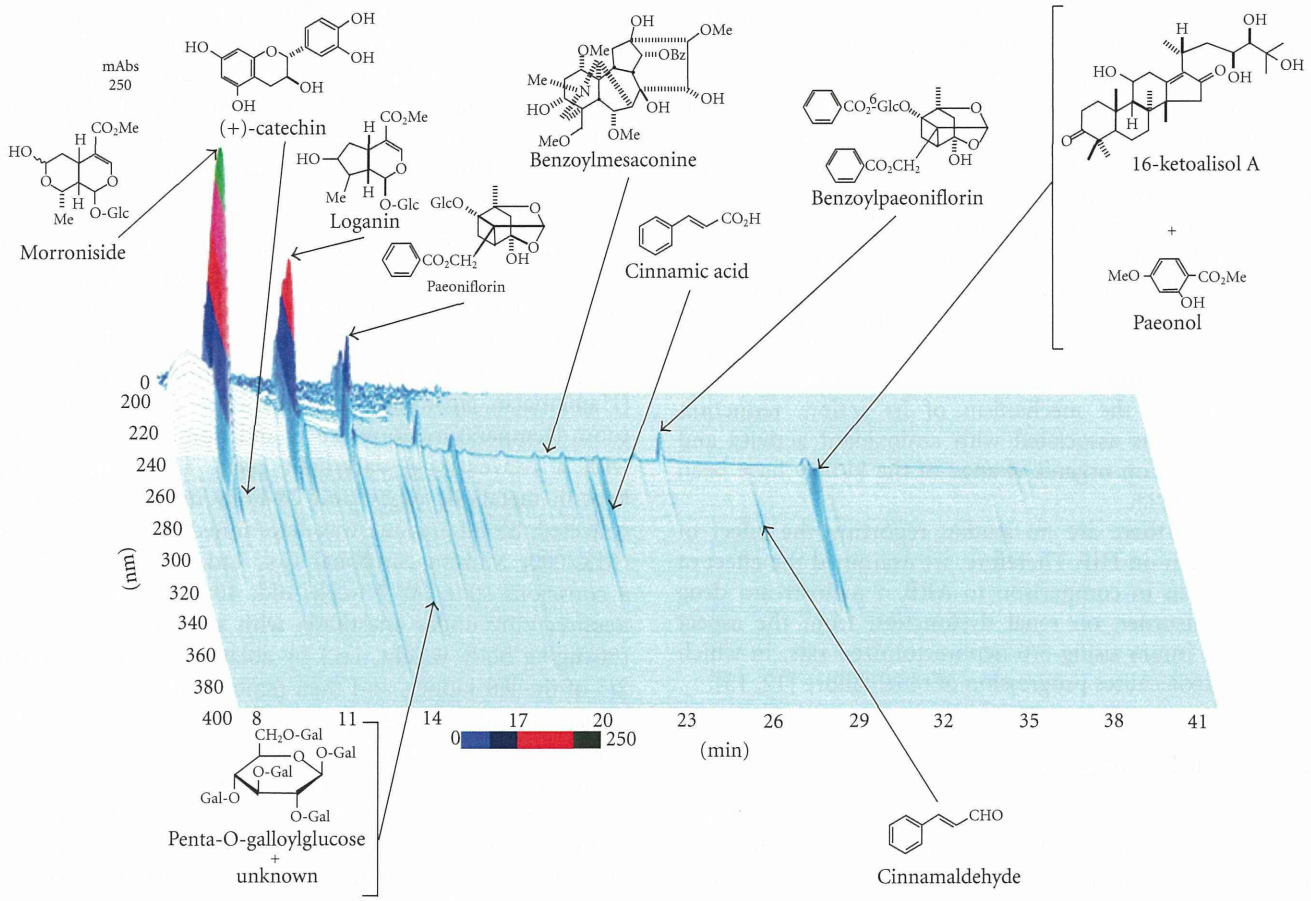

FIGURE 1: Chemical profile of hachimijiogan analyzed by three-dimensional HPLC.

2.5. Real-Time RT-PCR. Total RNA was prepared using the RNeasy Mini kit (QIAGEN, Valencia, CA, USA). First-strand cDNA was synthesized by SuperScript II reverse transcriptase (Invitrogen, Carlsbad, CA, USA). cDNA was amplified quantitatively using SYBR Premix Ex Taq (TaKaRa-Bio, Otsu, Japan). The primer sequences are summarized in Table 1. Real-time quantitative RT-PCR was performed using an ABI Prism 7300 sequence detection system (Applied Biosystems, Foster City, CA, USA). All data were normalized to β-actin mRNA.

2.6. Protein Preparation and Western Blotting. The cortex was dissected from the frozen kidney and homogenized in buffer A (10 mM HEPES pH 7.9, 10 mM KCl, 0.1 mM EDTA, 0.1 mM EGTA, 1 mM DTT, 1 mM PMSF, 20 mM β-glycerophosphate, 0.1 mM sodium orthovanadate, 10 μg/mL aprotinin, and 10 μg/mL leupeptin) and chilled on ice for 15 min. Next, 25 μL of 10% Nonidet P-40 was added and the suspension was vigorously vortexed for 10 s and kept on ice for 5 min. The nuclear pellets were washed with 100 μL of buffer A and suspended in 50 μL of buffer C (20 mM HEPES pH 7.9, 0.4 M NaCl, 1 mM EDTA, 1 mM EGTA, 1 mM DTT, 1 mM PMSF, 20 mM β-glycerophosphate, 1 mM sodium orthovanadate, 10 μg/mL aprotinin, 10 μg/mL leupeptin). The mixture was kept on ice for 15 min with frequent agitation. Nuclear extracts were prepared by centrifugation at 15,000 rpm for 5 min.

Kidney lysates were resolved by SDS-PAGE and transferred to Immobilon-P nylon membrane (Millipore, Bedford, MA, USA). The membrane was treated with BlockAce (DS pharma Co. Ltd., Suita, Japan) overnight at 4°C and probed with primary antibodies. An antibody against HIF-1α (H1alpha67) was purchased from Abcam (Cambridge, UK). Lamin B was used as an internal control. Antibodies against Lamin B (C-20) were purchased from Santa Cruz Biotechnologies (Santa Cruz, CA, USA). Enhancer solutions (Can Get Signal; Toyobo, Osaka, Japan) were used for the dilution. The antibodies were detected using horseradish peroxidase-conjugated antimouse and antigoat IgG (Dako Cytomation, Glostrup, Denmark) and visualized with the ECL system for Lamin B and ECL-plus for HIF-1α (GE Healthcare, Buckinghamshire, UK).

2.7. Histology and Immunohistochemistry. Rats were deeply anesthetized by an intraperitoneal injection of pentobarbital sodium (50 mg/kg body weight). Kidney was rapidly excised and immediately immersed in 4% paraformaldehyde and embedded in paraffin. Sections (5 μm thick) were routinely stained with hematoxylin and eosin. Mouse monoclonal antibody against HIF-1α (H1alpha, 1 : 25 diluted; Novus

Table 1: Sequences for RT-PCR primers.

Genes	Forward	Reverse
β-actin	GCCAACCGTGAAAAGATGAC	AGGCATACAGGGACAACACA
VEGF	TTACTGCTGTACCTCCAC	ACAGGACGGCTTGAAGATA [12]
Glut-1	AGGTGTTCGGCTTAGACTC	GAAGGGCAACAGGATACAC

VEGF: vascular endothelial growth factor, Glut-1: glucose transporter 1.

Biologicals, Littleton, CO, USA) was used for immunohistochemical staining of kidney as previously described [14]. For detecting primary antibodies on rat tissue specimens, M.O.M. kit (Vector, Burlingame, CA, USA) was used for special blocking. Tissue sections were cut at 5 micrometers from tissue blocks and placed on slides. After deparaffinization, sections were soaked in target retrieval solution (TRS, pH 6.1, Dako Cytomation) in a nonmetal-containing plastic-made pressure cooker and irradiated in a microwave oven for 15 minutes (maximum 500 W). After irradiation, sections were rinsed under running water for 2 minutes, soaked in 3% H_2O_2 methanol solution for 5 minutes, and then soaked in 5% BSA for 1 minute. After that, M.O.M. mouse Ig blocking reagent was applied and incubated for 1 hour. Primary antibody was diluted to a previously determined optimal concentration in M.O.M. diluent. The diluted antibody was applied to the tissue sections in a moist chamber and irradiated intermittently for 30 minutes (250 W, 4 seconds on, 3 seconds off). After three washes with Tris-buffered saline containing 1% Tween (TBS-T) for 5 minutes, peroxidase-conjugated Envision kit for mouse (Envision-PO, Envision System, Dako Cytomation) was used on the appropriate specimens in the moist chamber. Irradiation was then performed intermittently for 30 minutes as described above. After washing 5 times with TBS, the sections were immersed in DAB solution (Sigma-Aldrich, St. Louis, MO, USA) with H_2O_2 and counterstained with hematoxylin (Dako Cytomation) and mounted under coverslips.

Immunopositivity for HIF-1α in the tubular cells of the cortex was counted using 18 fields per group, and the average number per field was determined.

2.8. Statistical Analysis. All values were presented as mean $\pm$ S.D., and were analyzed by one-way analysis of variance (ANOVA) followed by Dunnett's test. $P < .05$ was accepted as statistically significant.

3. Results

3.1. Body Weight, Kidney Weight, Blood Pressure, and Urinary Volume. Table 2 shows the changes in body weight, kidney weight, blood pressure and urinary volume of the rats during the 1-week experimental period. The final body weights of the 5/6Nx groups were significantly lower than that of the sham group. There were no significant differences between baseline and final body weights in the 5/6Nx groups. The remnant kidney weights among the 5/6Nx groups did not change after the 1-week treatment. Blood pressures among all groups also did not change during the 1-week treatment. Urinary volumes of the 5/6Nx groups increased significantly compared to the sham group. There were no significant differences between baseline and final urinary volumes in the 5/6Nx groups.

3.2. Serum and Urine Biochemical Parameters. Table 3 shows the effects of hachimijiogan on serum and urine biochemical parameters. BUN levels of the control and low-dose hachimijiogan groups were significantly higher than that of the sham group. There were no significant differences in BUN levels among the four 5/6Nx groups. The s-Cre level of the control group was significantly higher than that of the sham group. There were no significant differences in s-Cre levels among the four 5/6Nx groups. Urinary protein excretion of the control group was significantly increased compared to that of the sham group, and those of the high-dose hachimijiogan and candesartan cilexetil groups were significantly decreased compared to that of the control group. Ccr levels of the four 5/6Nx groups were significantly decreased compared to that of the sham group. The 8-OHdG level of the control group was significantly higher than that of the sham group, and those of the low-dose hachimijiogan, high-dose hachimijiogan, and candesartan cilexetil groups were significantly lower than that of the control group.

3.3. Renal Cortical Hypoxia-Related Factors. The volumes of HIF-1α protein of the four 5/6Nx groups were significantly increased compared to that of the sham group, and that of the high-dose hachimijiogan group was significantly increased compared to that of the control group (Figure 2(a)). Figures 2(b) and 2(c) show the effects of hachimijiogan on renal mRNA levels of VEGF and glucose transporter-1 (Glut-1). In the high-dose hachimijiogan group, the mRNA levels of VEGF and Glut-1 were significantly increased compared to those of the sham and control groups.

Immunohistochemical studies also showed that the expression of HIF-1α of the high-dose hachimijiogan group was increased compared to that of the control group (Figures 3(a)–3(e)). There was a significantly large number of HIF-1α-positive cells in the high-dose hachimijiogan group compared to the control group (Figure 3(f)).

4. Discussion

Recently, as a final common pathway of various renal diseases, attention has been focused on tubulointerstitial hypoxia. It has been reported that the hypoxia of renal tissue was caused by decreasing peritubular capillary blood flow due to renal fibrosis, abnormal production of vasoactive

Table 2: Physiological data of experimental animals.

Group	Body weight (g)		Kidney weight (g/100g BW)	Systolic blood pressure (mmHg)		Diastolic blood pressure (mmHg)		Urine volume (mL/day)	
	Baseline	Final		Baseline	Final	Baseline	Final	Baseline	Final
Sham	297.1 ± 11.0	325.5 ± 12.0	0.311 ± 0.04	121.4 ± 14.2	113.7 ± 10.8	56.4 ± 13.5	62.6 ± 16.2	5.7 ± 3.1	6.4 ± 2.8
Control	261.7 ± 22.9	291.6 ± 26.4*	0.331 ± 0.05	124.3 ± 5.8	127.7 ± 8.2	69.7 ± 6.7	59.1 ± 12.2	20.3 ± 6.6**	21.1 ± 6.1**
LD-HJG	253.6 ± 17.6	275.9 ± 24.3*	0.341 ± 0.03	132.9 ± 27.1	130.0 ± 17.2	74.2 ± 19.1	62.8 ± 16.2	17.6 ± 6.7**	14.1 ± 6.3**
HD-HJG	257.5 ± 16.6	295.6 ± 16.4*	0.354 ± 0.04	122.8 ± 15.6	126.3 ± 8.9	70.1 ± 17.3	56.9 ± 6.1	20.6 ± 8.3**	18.0 ± 7.1**
Candesartan	264.3 ± 14.6	276.1 ± 16.6*	0.343 ± 0.03	121.4 ± 14.6	119.7 ± 16.2	70.9 ± 15.8	58.5 ± 13.1	20.2 ± 13.4**	16.5 ± 12.8**

LD-HJG: low-dose hachimijiogan; HD-HJG: high-dose hachimijiogan.
Baseline: before drug administration; Final: after 1 week of drug administration.
Data represent mean ± S.D. ($n = 8$–10). $^{*}P < .05$, $^{**}P < .01$ versus sham group.

Table 3: Effect of hachimijiogan on renal functional parameters.

	s-Alb (mg/dL)	BUN (mg/dL)	s-Cre (mg/dL)	u-Pro (mg/day)	Ccr (mL/min/kg BW)	8-OHdG (ng/day)
Sham	834.8 ± 110.9	15.6 ± 1.9	0.32 ± 0.14	13.01 ± 7.29	5.03 ± 3.07	325.9 ± 106.5
Control	887.1 ± 67.4	50.6 ± 36.7**	1.44 ± 1.32**	35.34 ± 20.62**	1.88 ± 0.94**	840.4 ± 252.4**
LD-HJG	895.8 ± 25.7	42.0 ± 27.1*	0.93 ± 0.59	25.15 ± 15.32	2.13 ± 1.40**	582.9 ± 201.8#
HD-HJG	833.9 ± 82.2	39.6 ± 25.7	0.87 ± 0.61	19.73 ± 5.41#	2.11 ± 0.86**	550.9 ± 210.5#
Candesartan	840.8 ± 92.5	33.8 ± 12.3	0.88 ± 0.49	15.41 ± 5.92##	1.65 ± 0.64**	484.2 ± 171.3##

LD-HJG: low-dose hachimijiogan; HD-HJG: high-dose hachimijiogan.
Data represent mean ± S.D. ($n = 8$–10).
$^{*}P < .05$, $^{**}P < .01$ versus sham group.
$^{\#}P < .05$, $^{\#\#}P < .01$ versus control group.

substance, anemia, and so on [15]. HIF, a heterogeneous nuclear ribonucleoprotein, is an important defense factor against tissue hypoxia. Activation of HIF and numerous downstream target genes protect tissues from hypoxia [6]. Under normoxic conditions, HIF-1α subunit is hydroxylated by prolyl hydroxylase (PHD). Hydroxylation is promoted by von Hippel-Lindau tumor suppressor protein binding to HIF-1α subunit. As a result, HIF-1α subunit is destroyed by proteasome. As PHD activity is decreased under hypoxic condition, HIF-1α subunit heterodimerizes with the constitutively expressed HIF-1β subunit. The heterodimeric HIF translocates into the nucleus, activating gene transcriptions, such as angiogenesis, cell metabolism, cell growth, apoptosis, and so on [16]. However, it has been reported that activation of HIF becomes less responsive to renal hypoxia in advanced renal dysfunction [17, 18]. It has also been reported that oral administration of cobalt chloride, which activates HIF, ameliorates renal injury in diabetic nephropathy of SHR/NDmer-cp rats [7], and that VEGF plays an important role in capillary repair in damaged glomeruli in glomerulonephritis rats induced by injection of anti-Thy-1.1 antibody [8]. On the basis of these reports, it is suggested that the treatments against hypoxia are useful for suppressing the progression of CKD.

The 5/6 nephrectomized rats we used in this study are a typical model of progressive renal disease. The initial change in this model causes increasing glomerular capillary pressure associated with a relative decrease in the expansion of efferent arterioles, resulting in glomerular hyperfiltration and hypertension. Glomerular hyperfiltration activates the renin-angiotensin system, eventually leading to glomerular sclerosis [19]. However, it has been reported recently that the deterioration of renal function in this model is correlated with an interstitial damage rather than a glomerular damage, and that chronic tissue hypoxia due to the initial reduction of blood flow causes the progression of renal failure [12]. Furthermore, it has been reported that the continuous infusion of dimethyloxalylglycine (DMOG), an activator of HIF, suppressed the increase of proteinuria in this model [20].

There have been some reports regarding the protective effects of hachimijiogan on renal function. Hachimijiogan had antihypertensive and renal-protective effects on Dahl salt-sensitive hypertensive rats, and its mechanism was suspected to enhance the production of prostaglandin E_2 [21]. Hachimijiogan had protective effects on diabetic nephropathy rats induced by streptozotocin injection, with its mechanism being suspected of improving lipid metabolism, glucose metabolism, and oxidative stress [22]. Hachimijiogan had renal-protective effects by improving oxidative stress and suppressing expression of fibronectin and TGF-β in spontaneously diabetic nephropathy rats [10]. Hachimijiogan also had renal-protective effects on 5/6 nephrectomized rats by a mechanism thought to reduce uremic toxins associated with oxidative stress [11]. Morroniside is a main component of Corni Fructus, which is contained in hachimijiogan, and was reported to have a renal-protective effect on diabetic

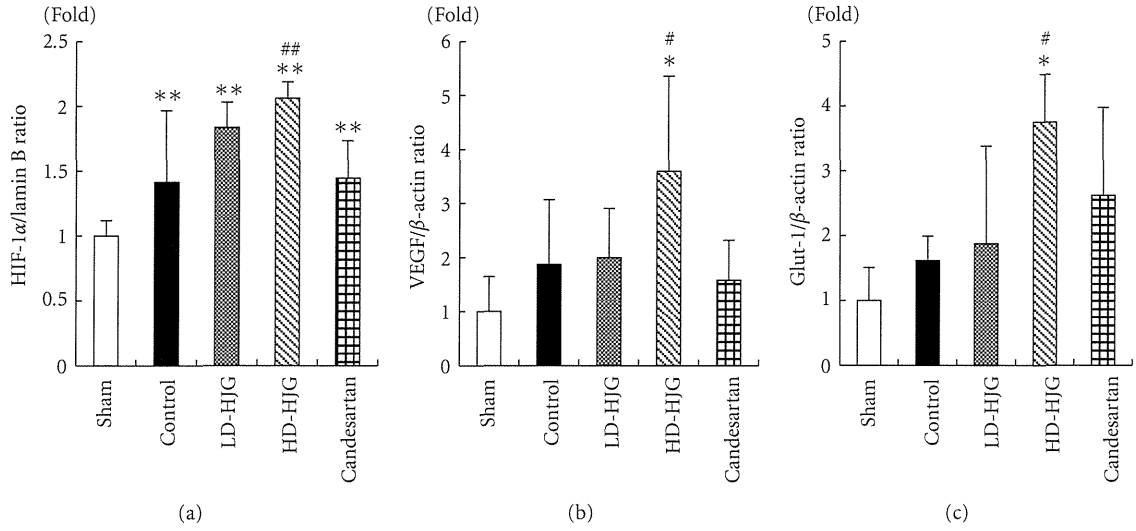

FIGURE 2: Measurement of renal cortical hypoxia-related factors in remnant kidney treated with hachimijiogan. The volume of HIF-1α protein of the four 5/6Nx groups increased significantly compared to that of the sham group, and that of the high-dose hachimijiogan group increased significantly compared to that of the control group (a). The mRNA levels of VEGF and Glut-1 of the high-dose hachimijiogan group increased significantly compared to those of the sham and control groups (b, c). (a) HIF-1α protein, (b) VEGF mRNA, (c) Glut-1 mRNA, LD-HJG: low-dose hachimijiogan, HD-HJG: high-dose hachimijiogan. Data represent mean ± S.D. ($n = 8$–10). $^{*}P < .05$, $^{**}P < .01$ versus sham group, $^{\#}P < .05$, $^{\#\#}P < .01$ versus control group.

nephropathy rats by inhibiting the production of advanced glycation end product and oxidative stress [23].

In this study, the levels of BUN, s-Cre, and urinary protein excretion of the control group were significantly higher than those of the sham group whereas the level of Ccr of the control group significantly decreased compared to that of the sham group. The HIF-1α protein level of the control group increased compared to that of the sham group one week after nephrectomy, as previously reported [12].

On the other hand, administration of high-dose hachimijiogan significantly reduced urinary protein excretion and elevated the HIF-1α protein level in the renal cortex. Therefore, it was suggested that hachimijiogan had an activating effect on HIF. This was also supported by the observations of increased VEGF mRNA and Glut-1 mRNA. Immunohistological examination of renal tubular epithelial cells also showed an increase in HIF-1α by the administration of hachimijiogan.

Administration of candesartan cilexetil, which has renal-protective effects [24, 25], significantly decreased urinary protein excretion. However, the HIF-1α protein level and the expressions of VEGF mRNA and Glut 1 mRNA did not increase by candesartan cilexetil administration. It had been reported that HIF activation in renal tissue decreases by the administration of candesartan cilexetil [12]. It is supposed that the main mechanism contributing to the attenuation of proteinuria by the administration of ARB is a reduction in glomerular capillary pressure, as previously reported [26].

It has already been reported that oxidative stress increased in patients with CKD [27]. In the state of uremia, due to the increase of reactive oxygen species in the vascular endothelium, a reduction in glutathione [28] and an increase in releasing reactive oxygen species from leukocytes [29] have been reported. It has also been reported that the activation of the renin-angiotensin system suppresses the expression of super oxide dismutase (SOD) [30]. This oxidative stress has been reported to have the possibility of inhibiting the activation of HIF [31]. Therefore, the involvement of oxidative stress was examined by measuring urinary 8-OHdG. The results showed that, compared with the sham group, the control group had a significantly increased level of urinary 8-OHdG, and the hachimijiogan and candesartan cilexetil groups had significantly decreased levels of urinary 8-OHdG. The antioxidant effects of hachimijiogan have been reported [10, 11]. Although ARB has also been reported to have antioxidant activity [32], the HIF activation in the candesartan cilexetil group did not increase in this study. Therefore, the mechanism of increasing HIF of the hachimijiogan group was considered to be a direct effect of hachimijiogan.

There are various reports about natural products that have an effect on HIF activation [33]. Concerning phenolic compounds, quercetin, contained in red wine, has been reported to have the effect of HIF activation on cultured murine brain endothelial cells in normoxia [34]. Green tea extract and its major component epigallocatechin gallate (EGCG) have been reported to activate HIF in human prostate cancer cells (PC-3ML) by inhibiting the degradation with PHD [35]. However, EGCG has also been reported to have a suppressive effect on HIF activation in HeLa cells and HepG2 cells by inhibiting the PI3K-AKT-mTOR pathway [36]. It is suggested that the activations of HIF and VEGF depend on the kinds of cultured cells or culture conditions. Moreover, there are as yet few reports on the study of the activation of HIF in vivo.

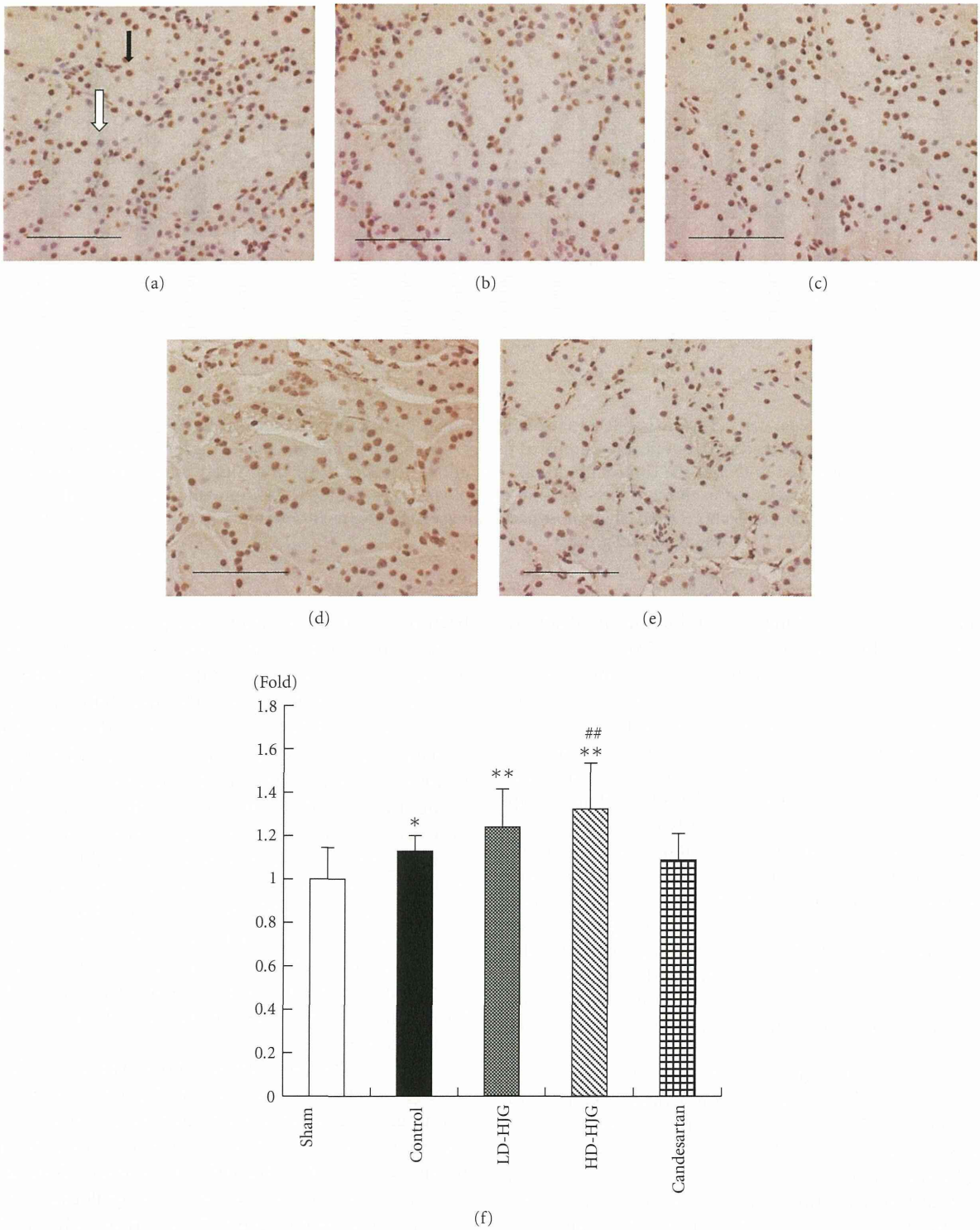

FIGURE 3: Immunohistochemical studies showed that the expression of HIF-1α of the high-dose hachimijiogan group increased compared to that of the control group (a–e). The black arrow indicates an HIF-1α-positive cell stained brown, and the white arrow indicates an HIF-1α-negative cell stained blue. The number of HIF-1α-positive cells in the high-dose hachimijiogan group increased significantly compared to that in the control group. (a) sham, (b) control, (c) low-dose hachimijiogan, (d) high-dose hachimijiogan, (e) candesartan cilexetil. (magnification 400x, scale bar: 100 μm), (f) Comparison with percentage of HIF-1α-positive cells/field in the every group. Data represent mean ± S.D. $^{*}P < .05$, $^{**}P < .01$ versus sham group, $^{\#\#}P < .01$ versus control group.

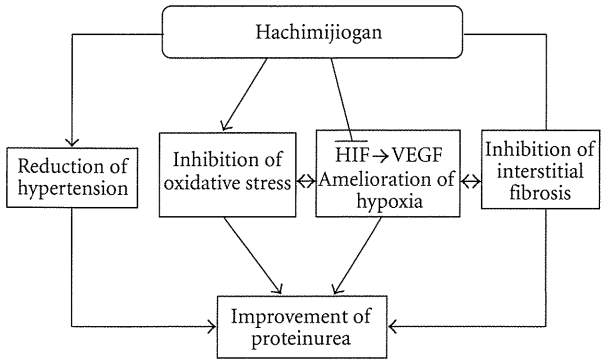

FIGURE 4: Hypothetical representation of the effects of hachimijiogan on renal dysfunction.

5. Conclusion

It has been suggested that hachimijiogan has a renal-protective effect through the influence of HIF activation. We summarized our hypothetical representation that explains the effects of hachimijiogan on renal dysfunction in Figure 4. Further experiments are needed to determine the active components and the mechanisms of the activation of HIF, and to study the long-term effects of hachimijiogan in vivo. Meanwhile, in terms of renal treatment via HIF, the hachimijiogan treatment is considered as a new therapeutic tool in addition to the existing renal treatments.

Acknowledgments

The authors are grateful to Mr. Arndt Gerz and Mr. Thomas Fenwick for assisting with the English version of the paper. This paper was supported by a Grant-in-Aid for Scientific Research (C) (no. 21590758) by the Japan Society for the Promotion of Science (JSPS).

References

[1] A. S. Go, G. M. Chertow, D. Fan, C. E. McCulloch, and C. Y. Hsu, "Chronic kidney disease and the risks of death, cardiovascular events, and hospitalization," *New England Journal of Medicine*, vol. 351, no. 13, pp. 1296–1305, 2004.

[2] M. J. Lysaght, "Maintenance dialysis population dynamics: current trends and long-term implications," *Journal of the American Society of Nephrology*, vol. 13, supplement 1, pp. S37–S40, 2001.

[3] G. Remuzzi and T. Bertani, "Pathophysiology of progressive nephropathies," *New England Journal of Medicine*, vol. 339, no. 20, pp. 1448–1456, 1998.

[4] L. G. Fine, D. Bandyopadhay, and J. T. Norman, "Is there a common mechanism for the progression of different types of renal diseases other than proteinuria? Towards the unifying theme of chronic hypoxia," *Kidney International, Supplement*, vol. 57, no. 75, pp. S22–S26, 2000.

[5] K. U. Eckardt, C. Rosenberger, J. S. Jürgensen, and M. S. Wiesener, "Role of hypoxia in the pathogenesis of renal disease," *Blood Purification*, vol. 21, no. 3, pp. 253–257, 2003.

[6] J. Marx, "How cells endure low oxygen," *Science*, vol. 303, no. 5663, pp. 1454–1456, 2004.

[7] S. Ohtomo, M. Nangaku, Y. Izuhara, S. Takizawa, C. Y. Strihou, and T. Miyata, "Cobalt ameliorates renal injury in an obese, hypertensive type 2 diabetes rat model," *Nephrology Dialysis Transplantation*, vol. 23, no. 4, pp. 1166–1172, 2008.

[8] Y. Masuda, A. Shimizu, T. Mori et al., "Vascular endothelial growth factor enhances glomerular capillary repair and accelerates resolution of experimentally induced glomerulonephritis," *American Journal of Pathology*, vol. 159, no. 2, pp. 599–608, 2001.

[9] K. Terasawa, "Kampo: Japanese-Oriental Medicine, insights from clinical cases," *K.K. Standard McIntyre*, pp. 243–244, 1993.

[10] T. Nakagawa, T. Yokozawa, N. Yamabe et al., "Long-term treatment with Hachimi-jio-gan attenuates kidney damage in spontaneously diabetic WBN/Kob rats," *Journal of Pharmacy and Pharmacology*, vol. 57, no. 9, pp. 1205–1212, 2005.

[11] N. Yamabe, T. Yokozawa, H. Y. Kim, and E. J. Cho, "Protective effect of Hachimi-jio-gan against renal failure in a subtotal nephrectomy rat model," *Journal of Pharmacy and Pharmacology*, vol. 57, no. 12, pp. 1637–1644, 2005.

[12] K. Manotham, T. Tanaka, M. Matsumoto et al., "Evidence of tubular hypoxia in the early phase in the remnant kidney model," *Journal of the American Society of Nephrology*, vol. 15, no. 5, pp. 1277–1288, 2004.

[13] T. Tanaka, I. Kojima, T. Ohse et al., "Cobalt promotes angiogenesis via hypoxia-inducible factor and protects tubulointerstitium in the remnant kidney model," *Laboratory Investigation*, vol. 85, no. 10, pp. 1292–1307, 2005.

[14] T. Kumada, K. Tsuneyama, H. Hatta, S. Ishizawa, and Y. Takano, "Improved 1-h rapid immunostaining method using intermittent microwave irradiation: practicability based on 5 years application in Toyama Medical and Pharmaceutical University Hospital," *Modern Pathology*, vol. 17, no. 9, pp. 1141–1149, 2004.

[15] M. Nangaku and K. U. Eckardt, "Hypoxia and the HIF system in kidney disease," *Journal of Molecular Medicine*, vol. 85, no. 12, pp. 1325–1330, 2007.

[16] R. H. Wenger, D. P. Stiehl, and G. Camenisch, "Integration of oxygen signaling at the consensus HRE," *Science's STKE*, vol. 2005, no. 306, p. re12, 2005.

[17] P. Katavetin, T. Miyata, R. Inagi et al., "High glucose blunts vascular endothelial growth factor response to hypoxia via the oxidative stress-regulated hypoxia-inducible factor/hypoxia-responsible element pathway," *Journal of the American Society of Nephrology*, vol. 17, no. 5, pp. 1405–1413, 2006.

[18] P. Katavetin, R. Inagi, T. Miyata et al., "Albumin suppresses vascular endothelial growth factor via alteration of hypoxia-inducible factor/hypoxia-responsive element pathway," *Biochemical and Biophysical Research Communications*, vol. 367, no. 2, pp. 305–310, 2008.

[19] T. H. Hostetter, J. L. Olson, H. G. Rennke, M. A. Venkatachalam, and B. M. Brenner, "Hyperfiltration in remnant nephrons: a potentially adverse response to renal ablation," *Journal of the American Society of Nephrology*, vol. 12, no. 6, pp. 1315–1325, 2001.

[20] Y. R. Song, S. J. You, Y. M. Lee et al., "Activation of hypoxia-inducible factor attenuates renal injury in rat remnant kidney," *Nephrology Dialysis Transplantation*, vol. 25, no. 1, pp. 77–85, 2010.

[21] N. Hirawa, Y. Uehara, Y. Kawabata et al., "Hachimi-jio-gan extract protects the kidney from hypertensive injury in dahl salt-sensitive rat," *American Journal of Chinese Medicine*, vol. 24, no. 3-4, pp. 241–254, 1996.

[22] T. Yokozawa, N. Yamabe, E. J. Cho, T. Nakagawa, and S. Oowada, "A study on the effects to diabetic nephropathy of hachimi-jio-gan in rats," *Nephron Experimental Nephrology*, vol. 97, no. 2, pp. e38–e48, 2004.

[23] N. Yamabe, K. S. Kang, E. Goto, T. Tanaka, and T. Yokozawa, "Beneficial effect of Corni Fructus, a constituent of Hachimi-jio-gan, on advanced glycation end-product-mediated renal injury in streptozotocin-treated diabetic rats," *Biological and Pharmaceutical Bulletin*, vol. 30, no. 3, pp. 520–526, 2007.

[24] K. Ueshima, S. Yasuno, K. Oba et al., "Impact of left ventricular hypertrophy on the time-course of renal function in hypertensive patients: a subanalysis of the CASE-J trial," *Circulation Journal*, vol. 74, no. 10, pp. 2132–2138, 2010.

[25] P. Morsing, "Candesartan: a new-generation angiotensin II AT receptor blocker: pharmacology, antihypertensive efficacy, renal function, and renoprotection," *Journal of the American Society of Nephrology*, vol. 10, supplement 11, pp. S248–S254, 1999.

[26] H. Rincon-Choles, B. S. Kasinath, Y. Gorin, and H. E. Abboud, "Angiotensin II and growth factors in the pathogenesis of diabetic nephropathy," *Kidney International, Supplement*, vol. 62, no. 82, pp. S8–S11, 2002.

[27] E. Dounousi, E. Papavasiliou, A. Makedou et al., "Oxidative stress is progressively enhanced with advancing stages of CKD," *American Journal of Kidney Diseases*, vol. 48, no. 5, pp. 752–760, 2006.

[28] L. Dou, N. Jourde-Chiche, V. Faure et al., "The uremic solute indoxyl sulfate induces oxidative stress in endothelial cells," *Journal of Thrombosis and Haemostasis*, vol. 5, no. 6, pp. 1302–1308, 2007.

[29] S. Sela, R. Shurtz-Swirski, M. Cohen-Mazor et al., "Primed peripheral polymorphonuclear leukocyte: a culprit underlying chronic low-grade inflammation and systemic oxidative stress in chronic kidney disease," *Journal of the American Society of Nephrology*, vol. 16, no. 8, pp. 2431–2438, 2005.

[30] W. J. Welch, J. Blau, H. Xie, T. Chabrashvili, and C. S. Wilcox, "Angiotensin-induced defects in renal oxygenation: role of oxidative stress," *American Journal of Physiology*, vol. 288, no. 1, pp. H22–H28, 2005.

[31] C. Rosenberger, M. Khamaisi, Z. Abassi et al., "Adaptation to hypoxia in the diabetic rat kidney," *Kidney International*, vol. 73, no. 1, pp. 34–42, 2008.

[32] T. W. Kurtz and M. Pravenec, "Antidiabetic mechanisms of angiotensin-converting enzyme inhibitors and angiotensin II receptor antagonists: beyond the renin-angiotensin system," *Journal of Hypertension*, vol. 22, no. 12, pp. 2253–2261, 2004.

[33] D. G. Nagle and Y. D. Zhou, "Natural product-derived small molecule activators of hypoxia-inducible factor-1 (HIF-1)," *Current Pharmaceutical Design*, vol. 12, no. 21, pp. 2673–2688, 2006.

[34] W. J. Wilson and L. Poellinger, "The dietary flavonoid quercetin modulates HIF-1α activity in endothelial cells," *Biochemical and Biophysical Research Communications*, vol. 293, no. 1, pp. 446–450, 2002.

[35] R. Thomas and M. H. Kim, "Epigallocatechin gallate inhibits HIF-1α degradation in prostate cancer cells," *Biochemical and Biophysical Research Communications*, vol. 334, no. 2, pp. 543–548, 2005.

[36] Q. Zhang, X. Tang, Q. Lu, Z. Zhang, J. Rao, and A. D. Le, "Green tea extract and (-)-epigallocatechin-3-gallate inhibit hypoxia- and serum-induced HIF-1protein accumulation and VEGF expression in human cervical carcinoma and hepatoma cells," *Molecular Cancer Therapeutics*, vol. 5, no. 5, pp. 1227–1238, 2006.

A Phagocytotic Inducer from Herbal Constituent, Pentagalloylglucose Enhances Lipoplex-Mediated Gene Transfection in Dendritic Cells

Shinichiro KATO,[a] Keiichi KOIZUMI,*[,a] Miyuki YAMADA,[a] Akiko INUJIMA,[a] Nobuhiro TAKENO,[a] Tsuyoshi NAKANISHI,[b] Hiroaki SAKURAI,[a] Shinsaku NAKAGAWA,[c] and Ikuo SAIKI[a]

[a] *Division of Pathogenic Biochemistry, Institute of Natural Medicine, University of Toyama; 2630 Sugitani, Toyama 930–0194, Japan:* [b] *Laboratory of Hygienics, Gifu Pharmaceutical University; 5–6–1 Mitahora-higashi, Gifu 502–8585, Japan: and* [c] *Department of Biotechnology and Therapeutics, Graduate School of Pharmaceutical Sciences, Osaka University; Suita, Osaka 565–0871, Japan.* Received May 6, 2010; accepted August 19, 2010

Antigen-presenting cells are key vehicles for delivering antigens in tumor immunotherapy, and the most potent of them are dendritic cells (DCs). Recent studies have demonstrated the usefulness of DCs genetically modified by lipofection in tumor immune therapy, although sufficient gene transduction into DCs is quite difficult. Here, we show that *Paeoniae radix*, herbal medicine, and the constituent, 1,2,3,4,6-penta-*O*-galloyl-*β*-D-glucose (PGG), have an attractive function to enhance phagocytosis in murine dendritic cell lines, DC2.4 cells. In particular, PGG in combination with lipofectin (LPF) enhanced phagocytic activity. Furthermore, PGG enhanced lipofection efficacy in DC2.4 cells, but not in colorectal carcinoma cell lines, Colon26. In other words, PGG synergistically enhanced the effect of lipofectin-dependent phagocytosis on phagocytic cells. Hence, according to our data, PGG could be an effective aid in lipofection using dendritic cells. Furthermore, these findings provide an expectation that constituents from herbal plant enhance lipofection efficacy.

Key words dendritic cell; lipofection; 1,2,3,4,6-penta-*O*-galloyl-*β*-D-glucose; phagocytosis

Dendritic cells (DCs) play a pivotal role in initiating and controlling the T cell-dependent immune response.[1] Immature DCs, localized in non-lymphoid tissues, have optimal capabilities for antigen uptake, processing and the formation of peptide-major histocompatibility (MHC) complexes. Antigen uptake and some cytokines, for example, in the inflammatory environment, promote their maturation and migration to T cell areas of regional lymphoid tissues, where matured DCs strongly present MHC class I and II restricted peptides to naïve T cells, inducing an immune response and differentiation.[2,3] Because of these properties, DCs have been considered quite attractive immune cells to achieve gene transduction for DNA-based immunization in tumor immunotherapy[4—7] and many gene delivery methods have attempted to optimize transduction and transfection to human and murine dendritic cells.[8—10]

However, despite advances in the understanding of DC biology, the development of genetic immunization strategies using DC-transfected plasmid DNA has been limited by their low transfection efficiencies.[11] Currently, the most efficient method for DC transduction is infection using a viral vector based on poxvirus, lentivirus, and adenovirus,[8,12,13] but viral vectors may be associated with safety concerns and generally require DNA codon optimization to overcome poor gene expression.[14,15] An attractive alternative to vector-mediated delivery into DCs is lipofection, non-viral gene transduction. The main advantages of lipofection are its ability to transfect all types of nucleic acids in a wide range of cell types, its ease of use, reproducibility and low toxicity.[16] Furthermore, recent studies have demonstrated the usefulness of DCs genetically modified by lipofection in tumor immunotherapy,[17] while sufficient gene transduction to DCs is quite difficult.[18] Therefore, it is easily thought that more efficient (DNA-based) DC vaccine therapy could be developed by not only understanding DC immune biology but also finding methods or substances which enhance lipofection efficiency in DCs.

We have sought out immunomodulating compounds derived from herbal medicine or Kampo preparations (formulation) for cancer therapy, especially metastasis.[19,20] In this study, we found that 1,2,3,4,6-penta-*O*-galloyl-*β*-D-glucose (PGG), which is contained in *Paeoniae radix* (roots of Paeonie lactiflora),[21] enhanced phagocytosis in murine a denndritic cell line, DC2.4, especially in combination with lipofectin (LPF). Lipofectin reagent (LPF; Invitrogen, CA, U.S.A.) is a cationic liposome, mixture of *N*-[1-(2,3-dioleyloxy)propyl]-*n*,*n*,*n*-trimethylammonium chloride (DOTMA) and dioleoyl phosphotidylethanol amine (DOPE) at 1 : 1 (w/w), and is widely used as a device for transfection of RNA, DNA, oligonucleotide and protein.[22—26]

These results motivated us to explore the effect of PGG on DC2.4 cells. PGG is a naturally occurring polyphenolic compound contained in many medical plants[27,28] and a number of studies have reported that PGG exhibits diverse bioactivity, for example, anti-tumor, anti-oxidant, and anti-inflammatory effects.[29] However, the effect of PGG on the phagocytosis of dendritic cells (DCs) has not been investigated, while th effect of polyphenol and tannins (a polyphenol) on phagocytosis and dendritic cells have been investigated well.[30—32] Phagocytosed exogenous antigens complexed with LPF induce high-antigen presentation *via* MHC class I and II and cytotoxic T lymphocytes (CTLs).[33,34] Hence, PGG may be a powerful candidate for tumor immunetherapy because it enhances the phagocytic effect of DC2.4 cells.

On the other hand, we hypothesized that PGG could enhance lipofection efficacy and have a new application for lipofection on DCs because lipofection largely depends on the phagocytic effect,[35] therefore, the present study investigated the effect of PGG on lipofection efficacy in DC2.4 and bone marrow-derived dendritic cells (BMDCs). Moreover, to demonstrate whether the effect of PGG depends on phagocytosis, we also tested the effect on Colon 26, murine colorectal carcinoma cell line. According to our data, the enhancement of lipofection efficacy by PGG was specific for dendritic cells and PGG could be a seed compound of an effective aid

* To whom correspondence should be addressed. e-mail: kkoizumi@inm.u-toyama.ac.jp © 2010 Pharmaceutical Society of Japan

for lipofection.

MATERIALS AND METHODS

Reagents AIM-V and Opti-MEM were purchased from Invitrogen (Carlsbad, CA, U.S.A.)/ GIBCO BRL (Grand Island, New York, U.S.A.). The aqueous extraction from *Paeoniae radix* was performed, as previously mentioned.[36] Briefly, about 45 g dried and cut roots were brewed with 900 ml water. Then the filtrate was collected after filtration. The residue was boiled with 800 ml water again and added in the filtrate after filtration. The filtrate was lysophilized. The powder was stored at 4 °C. The concentration used in the experiment was based on the dry weight of the extract (mg/ml). 1,2,3,4,6-penta-*O*-galloyl-*β*-D-glucose (PGG) was purchased from Toronto Research Chemicals Inc. PGG stock solution, originally dissolved to a concentration of 5 mM in 100% dimethyl sulfoxide (DMSO). Paeoniflorin was purchased from Wako Pure Chemical Industries, Ltd. (Osaka, Japan) Paeoniflorin and Gallic acid (GA) stock solution originally dissolved to a concentration of 10 mM in distillated water. 1,3,6-tri-*O*-galloyl-*β*-D-glucose (TGG) stock solution originally dissolved to a concentration of 10 mM in 100% DMSO. These all chemical compounds were diluted to the desired concentration in AIM-V or Opti-MEM just before using.

Cell Culture DC2.4 cell, derived from a c57BL/6 immature dendritic cell line, was maintained in RPMI1640 supplemented with 50 μM β-melcaptoethanol. Colon26, derived from BALB/c colorectal cancer, was maintained with RPMI1640 supplemented with 2 mM L-glutamine. All media contained 10% fetal calf serum (FCS), 100 U/ml penicillin and 100 mg/ml streptomycin, and cultures were kept at 37 °C in a humidified atmosphere of 5% CO_2/95% air.

Phagocysosis in DC2.4 Fluorescence isothiocianate (FITC) conjugated-dextran (average molecular weight 40 kDa) was purchased from SIGMA-ALDRICH (St. Louis, MO, U.S.A.) and originally dissolved to a concentration of 10 mg/ml in balanced salt solution (BSS). Phagocytosis in DC2.4 was performed by modification of a previously reported method.[37] In this assay, AIM-V media was used instead of growth media. Briefly, 1×10^5 cells/well were seeded in a 24-well plate (Corning corter) and pre-incubated with PGG for 1.5 h at 37 °C. Pre-treated DC2.4 was phagocytosed in the presence of 10—500 μg/ml FITC-dextran or lipoplex for 1 h at 37 °C, which was made of FITC-dextran and 20 μl Lipofectin (Invitrogen) by co-incubation for 35 min. To inhibit phagocytosis of DC2.4 cells, DC2.4 cells were pre-incubated with wortmannin (final concentration; 5 μM) for 20 min before addition of FITC-dextran. FITC-positive cells were detected by fluorescence microscopy using a Keyence fluorescence microscope. For quantitative determinations of transfection efficiency, fluorescent cells were assessed by fluorescence-activated cell sorting (FACS) using a FACSCalibur flow cytometer (Becton-Dickinson, Mountain View, CA, U.S.A.) and CellQuest software.

Differentiation of Bone Marrow-Derived Dendritic Cells Bone marrow-derived dendritic cells (BMDCs) were differentiated from c57BL/6NCrSlc (9—10-weeks-old specific pathogen free female, Japan SLC (Hamamatsu, Japan)) as reported previously.[38] Differentiated BMDCs were qualified by immunophenotypes and phagocytic activity using FITC-dextran and we used defined BMDCs which express both CD11c and MHC class II more than 70% of total population.

Plasmids The vectors encoding green fluorescent protein (GFP) mutant, pEGFP-N1 and pEGFP-C1, were purchased from Clontech (Palo Alto, CA, U.S.A.). These vectors encode a mutant GFP that contains more than 190 silent nucleotide changes to optimize the coding sequence based on human codon-usage preferences,[39] and mutations at residue 64 (Phe→Leu) and 65 (Ser→Thr), which results in enhanced fluorescence and a single excitation peak at 488 nm.

Lipofection and Transgenes Expression Lipofection using a lipofectin reagent was performed by following the modified instructions of the manufacture. One day before transfection, 2×10^5 cells were seeded in growth media, and nearly 60% confluent cells were used for lipofection. Four microliters of lipofectin reagent was diluted in 100 μl Opti-MEM in one tube and incubated for 30 min at room temperature. Meanwhile, 2—4 μl pEGFP-N1 (1 μg/μl) and pEGFP-C1 (1 μg/μl) (Clontech) were diluted in 100 μl Opti-MEM in another tube separately for 15 min at room temperature. The transfection reagents and plasmid solution were then mixed and incubated at room temperature based on the manufacturer's instructions. Cells were familiarized with Opti-MEM for 30 min before lipofection. Eight-hundred microliters of Opti-MEM were added to the mixed solution (finally 200 μl+800 μl), then after removal of the conditioned Opti-MEM, cells were added to transfection solutions (1 ml) and incubated for 5 h. After lipofection for 5 h, transfection solution was replaced with growth media. In PGG-assisted lipofection, PGG was used for incubation of lipoplex throughout lipofection. Twenty-four hours following lipofection, enhanced green fluorescent protein (EGFP)-positive cells were detected and quantified by the same methods as for the phagocytosis of DC2.4.

Flow Cytometric Analysis and Immunophenotypic Analysis After removal of the supernatant, cells were split off using 0.13% trypsin and ethylenediaminetetraacetic acid (EDTA), pelleted by centrifugation, resuspended in phosphate buffered saline (PBS) containing 2% FCS to a final density of -5×10^6 cells/ml, and filtered through a nylon membrane to remove cell aggregates. Flow cytometry for EGFP and propidium iodide (PI) fluorescence were performed using a FACSCalibur (BD Bioscience). For immunophenotypic analysis of DC2.4 cells, split cells were suspended in FACS buffer ($0.5—1\times10^6$ cells/50 μl), containing PBS in 0.02% NaN_3 (w/v) and 2% FCS (v/v). Cells were first incubated with an antibody against FcRg (clone 2.4G2) for 5 min and then labeled with antibodies against CD80 (clone 16-10A1), CD86 (clone GL1), MHC class I (clone 28-14-8) and MHC class II (clone M5/114.15.2) for 30 min. All polyethylene (PE)-conjugated mAb were acquired from BD Biosciences.

Statistical Analysis Three means ($\pm$1 S.D.) were composed using analysis of variance (ANOVA) (Figs. 1, 3). Two means ($\pm$1 S.D.) were composed using the unpaired Student's *t*-test (two tailed) (Figs. 2, 4). A p value of less than 0.05 was considered significant.

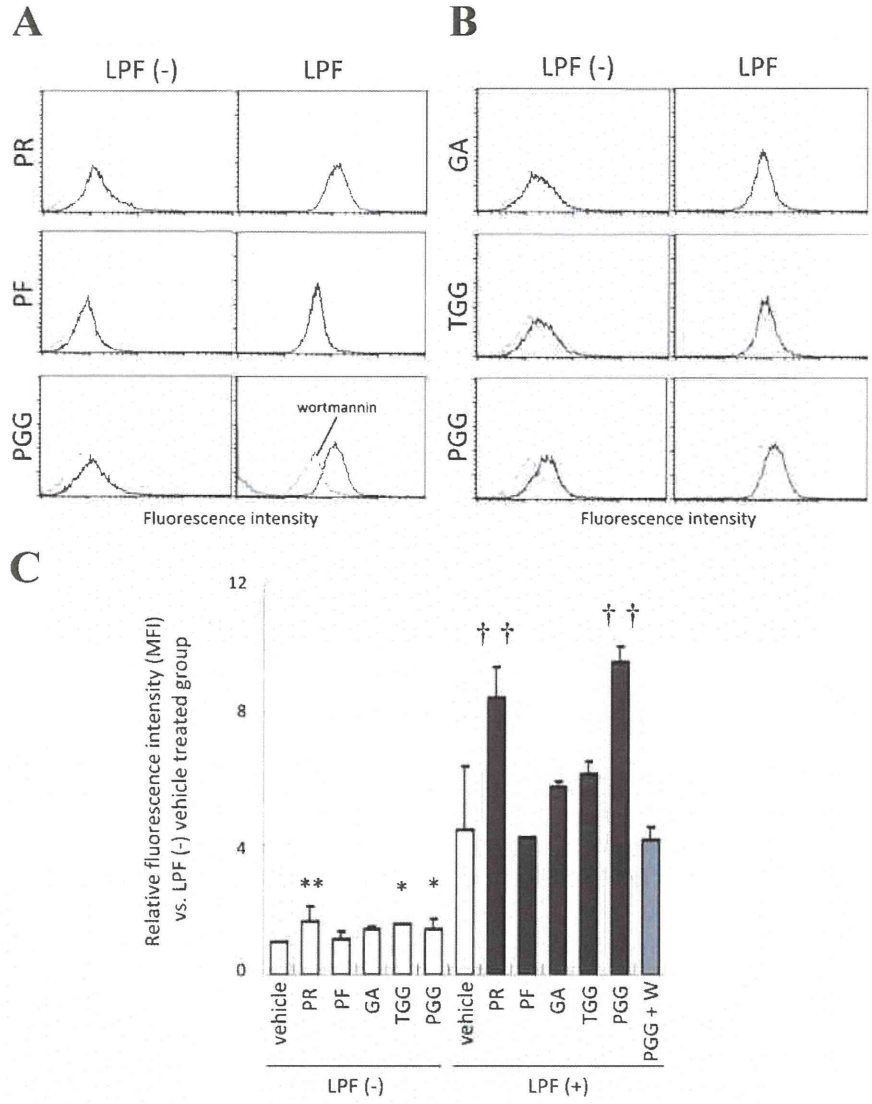

Fig. 1. Ability of 1,2,3,4,6-Penta-*O*-galloyl-*β*-D-glucose (PGG) to Phagocytose into DC2.4

After pre-incubation with (A) 1 mg/ml *Paeoniae radix* (PR), 10 mM Paeoniflorin (PF) or 10 mM PGG and (B) 10 mM gallic acid (GA), 10 mM 1,3,6-tri-*O*-galloyl-*β*-D-glucose (TGG) or 10 mM PGG for 1.5 h, DC2.4 phagosytosed for 1 h at 37 °C in the presense of 250 mg/ml FITC-dextran combined without (left) or with (right) Lipofectin (LPF). Phagocytosed DC2.4 were analyzed by flow cytometer. Filled profile, non-treated cells as control; gray dotted line, FITC-dextran without preincubation with indicated compounds; black line, FITC-dextran with preincubation with indicated compounds, FITC-dextran with preincubation with PGG and 5 *μ*M wortmannin (abbreviation; W) to inhibit phagocytosis. Data are representative of at least two independent experiments. (C) Relative mean fluorescence intensity (MFI) as phagocytic activity was assessed by flow cytometry. Data are presented as the means±S.D. of at least two independent experiments. $*p<0.05$, $**p<0.01$, *vs.* LPF (−) vehicle group, $\dagger\dagger p<0.01$, *vs.* LPF (+) vehicle group by analysis of variance (ANOVA) with Bonferroni correction.

RESULTS AND DISCUSSION

Phagocytosis in DC2.4 Cells Was Enhanced by 1,2,3,4,6-Penta-*O*-galloyl-*β*-D-glucose (PGG) Recently, we found that the ability of *Paeonie radix* (aqueous extractions) to engulf FITC-dextran into DC2.4 cells occurred in an FITC-dextran and *Paeonie radix* (PR) (Figs. 1A, C). To identify which chemical compounds enhanced engulfment in DC2.4 cells from *Paeonie radix*, we tested the effect of paeoniflorin (PF) and PGG, contained in PR,[27] on incorporation of FITC-dextran in DC2.4 cells. Of these compounds, PGG enhanced engulfment in DC2.4 cells at the same level as PR, while PF, which is the major compound contained in PR, hardly enhanced engulfment (Fig. 1A). PGG had little effect on engulfment with FITC-dextran alone but engulfment was apparently enhanced with the FITC-dextran/lipofectin (LPF) complex (Fig. 1C). The effect was cancelled by wortmannin, a phagocytosis inhibitor,[40] suggesting that the increase of intracellular FITC-dextran depended on the enhancement of phagocytic activity (Figs. 1A, C). This means that PGG synergistically enhances phagocytosis in combination with LPF in DC2.4 cells. In this property, PGG is utilized for lipofection using LPF. Furthermore, we also found the importance of the chemical structure of PGG in the enhancement of phagocytosis in DC2.4 cells (Figs. 1B, C). PGG has five ester bonds formed between the hydroxyl group of the glucose backbone and the carboxyl group of gallic acid (GA).[29] 1,3,6-Tri-*O*-galloyl-*β*-D-glucose (TGG), which has three ester bonds, enhanced the phagocytosis of DC2.4 in the absence of LPF and had a tendency to enhance

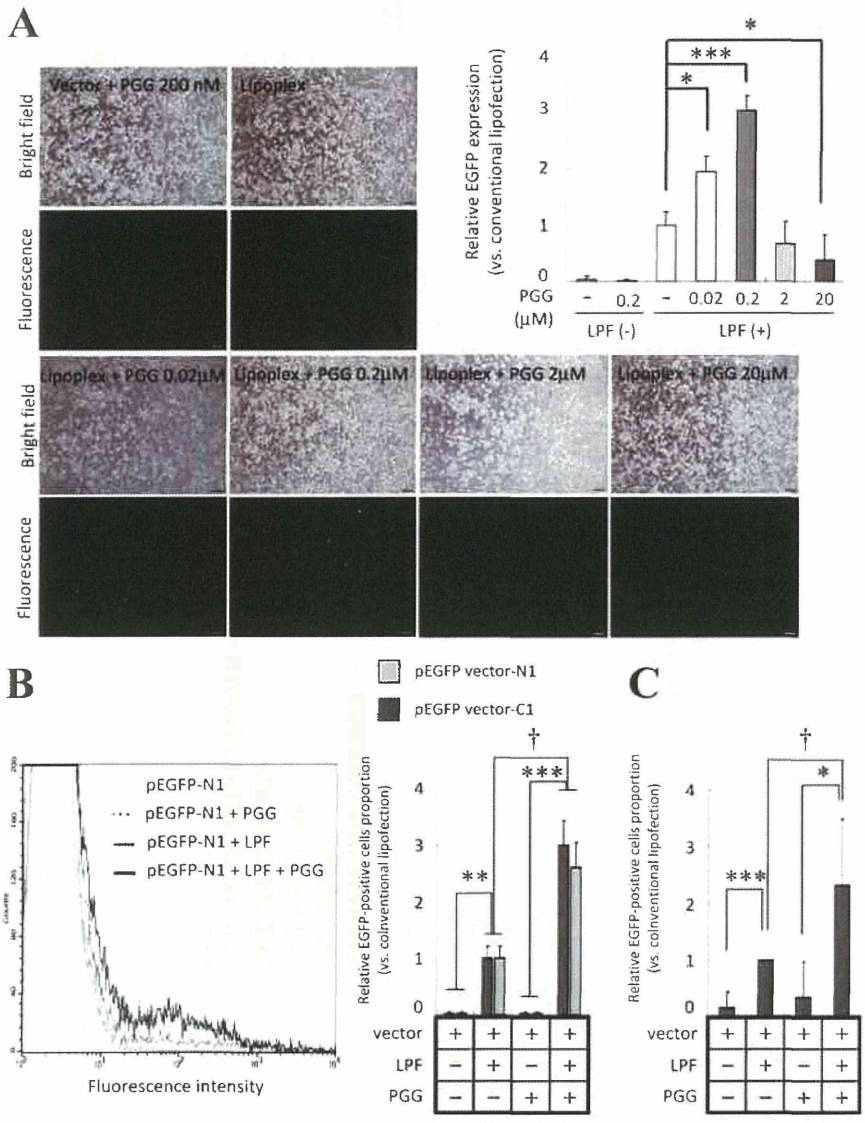

Fig. 2. Lipofection with Lipofectin (LPF) Combined with PGG in DC2.4 and Bone Marrow Derived Dendritic Cells

DC2.4 bone marrow derived dendritic cells were transfected with LPF and PGG together for 5 h. After 24 h of culture with growth medium at 37 °C, EGFP expression was obtained by fluorescence microscopy and flow cytometry. (A) Transfected DC2.4 cells with 2 μg pEGFP-N1 vector with 200 nM PGG (without Lipofection) (upper left), vector+LPF (lipoplex) (upper right), vector+LPF+PGG indicated concentration (lower panel). Up and downward square observe pictures under phase-contact microscopy and fluorescence image. Scale bar=100 μm. EGFP gene transduction of DC2.4 lipofected with indicated PGG concentration was expressed as EGFP expression (relative EGFP-positive cell proportion (fold)). (B) Histogram image shows EGFP intensity on DC2.4 cells transfected respectively. EGFP gene transduction of DC2.4 lipofected with indicated combination was expressed as EGFP expression (relative EGFP-positive cell proportion (fold)). (C) EGFP gene transduction of BMDCs lipofected with 4 μg pEGFP vector and indicated combination was expressed as EGFP expression (relative EGFP-positive cell proportion *vs.* conventional lipofection (fold)). Data are presented as the means±S.D. of (B) five or (C) three independent experiments. * $p<0.05$, ** $p<0.01$, *** $p<0.005$, *vs.* respective LPF-untreated group, † $p<0.01$, *vs.* PGG-untreated group by two-tail unpaired Student's *t*-test.

phagocytosis in the presence of LPF but the enhancement was lower than that of PGG. Additionally, GA also had a tendency to enhance phagocytosis, and the enhancement of GA was lower than that of TGG, suggesting that the ester binding mode between the glucose core and gallic acid rather than gallic acid itself is strongly involved in the enhancement of phagocytosis in DC2.4 cells (Fig. 1B).

Enhanced the Efficacy of Lipofection Using PGG in Mouse Dendritic Cells Gene transfer into DCs is critical for potential therapeutic applications as well as for study of the genetic basis of DC-mediated immunological development and immune regulation, however, transfection into DCs is difficult.[11] In particular, it is difficult to transduce naked or plasmid DNA on DCs.[9] The main advantages of lipofection are its ability to transfect all types of nucleic acids in a wide range of cell types, its ease of use, reproducibility and low toxicity,[16] therefore, development of more efficient lipofection must enable DC vaccine therapy, and knowledge of DCs biology should be disseminated.

Thus, we tested the effect of PGG on lipofection in DC2.4 cells because PGG enhanced phagocytic activity. In pilot studies of our lipofection, we determined the optimal concentrations of the transfection reagent, plasmid vector and the length of incubation required for the best expression of EGFP in DC2.4 cells. We basically performed lipofection according to the instructions of the manufactures using a GFP

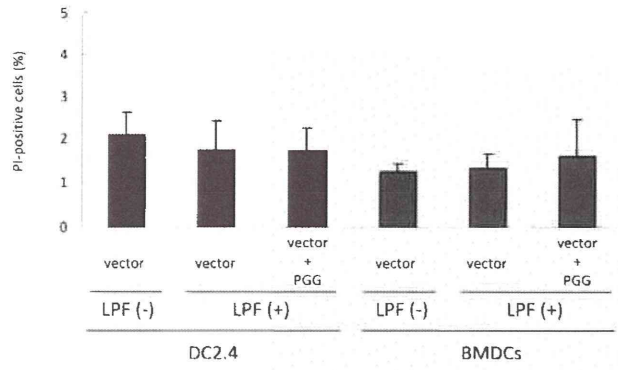

Fig. 3. Effect for Combination of Lipofectin (LPF) and 1,2,3,4,6-Penta-*O*-galloyl-β-D-glucose (PGG) in DC2.4 and BMDCs for Cell Viability

After 24 h of transfection, Propium iodide (PI) staining as DC2.4 and BMDCs viability was determined by flow cytometry. Data are presented as the means±S.D. of three independent experiments. No significant difference by ANOVA.

reporter construct, pEGFP-N1 and pEGFP-C1 vector to determine lipofection efficacy at 24 h posttransfection. For lipofection, we used 2 μg pEGFP-N1 or pEGFP-C1 vector as cytotoxicity (*i.e.*, cell detachment) was noted at higher amounts (data not shown) and 4 μl LPF. Lipofectin required an incubation period of >1 h with DC2.4 cells, whereas optimal results were obtained with about 5-h incubation in serum-free medium (EGFP-positive ($EGFP^+$) cells; 2.7±0.9%, n=5). Our lipofection efficacy corresponds to previous studies using lipofection in dendritic cells (lipofection efficacy is less than 2% or not detectable.).[9,41]

To evalutate the effect of PGG on lipofection, we used PGG in the preceding lipofection during incubation to prepare the pEGFP vector/LPF complex (lipoplex) for lipofection, and determined the efficacy of EGFP for lipofection efficacy by flow cytometry and fluorescent microscopy. PGG expectedly enhanced the expression of EGFP (Fig. 2) and enhancement was achived in a concentration-dependent manner, but more than 2 μM PGG did not enhance the expression of EGFP (Fig. 2A). Furthermore, DC2.4 cells transfected with pEGFP-N1 vector in combination with 200 nM PGG (without LPF) produced no detectable EGFP fluorescence. A similar phenomenon was also obtained for phagocytic activity in DC2.4 (Fig. 1). Hence, PGG synergistically enhanced phagocytosis and lipofection using LPF. A similar result was obtained using another vector, pEGFP-C1 (Fig. 2B). Thus, transfection activity in an immature dendritic cell line DC2.4 cells was highly enhanced by PGG.

To sophisticate and assess the function of PGG as an inducer of lipofection, we used bone marrow derived dendritic cells (BMDCs) instead of DC2.4 cells. BMDCs were evaluated by flowcytometer and phagocytic activity using FITC-dextran. BMDCs express both CD11c and MHC class II more than 70% of total population were used in our experiments and lipofection procedure on DC2.4 was also applied to BMDCs except for amount of plasmid vector, 2 μg plasmid vector changed to 4 μg. As a result, although the effect of PGG on lipofection efficacy in BMDCs did not seem to be strong, it was significantly enhanced (Fig. 2C). Therefore, PGG could enhance the lipofection efficacy in dendritic cell- or phagocytic cell-specific manner.

Effect of Lipofection with PGG on Dendritic Cells Viability In addition to measuring EGFP expression at 24 h posttransfection, we assessed the effect of lipofection combined with PGG on cell viability by staining with propium iodide (PI) and using a flow cytometer. In Fig. 3, DC2.4 and BMDCs were not damaged by lipofectin in combination with PGG, and 200 nM PGG by itself also did not exhibit cytotoxicity on these cells (determined using WST-1: cell proliferation assay; data not shown). PGG might not exhibit remarkable cytotoxicity because of the low concentration. Usually, non-viral transfections are harmful to DCs[9,17] and lipoplex can increase cytotoxicity along with lipofection efficacy in a dose-dependent manner.[42] Clinically, all vaccines and DNA-based DC vaccine therapies must be safe, therefore, PGG would be a useful aid for lipofection.

Does Lipofection in Combination with PGG Depend on Phagocytosis? We have suggested that PGG enhanced the effect of lipofection on DC2.4 cells and BMDCs, however, the action mechanism of PGG is still unclear. Although one possibility was shown that PGG enhanced phagocytic activity in DC2.4 cells (Fig. 1), it remained to be confirmed. PGG may also enhance lipofection efficacy by increasing phagocytic activity. In the next study, to determine whether the effect of PGG on lipofection depends on phagocytosis, we tested its effect using colon 26 cells, a murine colon carcinoma cell line. The endocytocytic lipoplex uptake pathway is further separated into phagocytosis (phagocytic cells) and pinocytosis (all cells).[43] As shown in Fig. 4, PGG slightly enhanced lipofection efficacy on colon 26 but not significantly, therefore, the enhancement of lipofection efficacy on DC2.4 and BMDCs by PGG greatly depend on intensified phagocytosis and is not implicated in the fusogenic effect. Namely, the effect of PGG would be restricted to phagocytic cells, like DCs.

The internalization mechanism of lipoplex is not well understood. An early report suggested that the fusogenic effect between the positively charged lipoplex and the plasma membrane is responsible for tranducing DNA into cytosol,[22] however, subsequent studies recently have shown the involvement of phagocytosis in delivering DNA.[44,45] Hence, it is currently believed along with this historical background that membrane fusion is important in lipofection but uptake of lipoplex largely depends on phagocytosis and endocytosis. According to our data, PGG specifically enhanced lipofection efficacy in DC2.4 cells and BMDCs. In other words, PGG enhanced some functions specifically found in DCs. Additionally, it was thought that phagocytosis facilitated by PGG enhanced lipofection efficacy.

A remaining question for our further study is which site of action of PGG is responsible for phagocytosis. In our lipofection protocol, PGG was added during the generation of lipoplex and transfection; namely, PGG affects lipoplex, DC2.4 or both to enhance lipofection efficacy.

If PGG modified lipoplex more effectively by making a lipoplex/PGG complex, PGG must enhance lipofection efficacy on colon 26 cells. It is unknown why they make a complex with each other, but the lipoplex/PGG complex must be phagocytosed through a DC-specific receptor. The recent identification of surface receptors expressed on DCs allow for a specific target for effective transfection.[46] Receptors such as FcγRI[47,48] and mannose[49,50] are attractive candidates for target cell surface molecules. If PGG has an affinity with